Theory of proximity effect in normal metal/$d_{x^2-y^2}$-wave superconductor interface in the presence of subdominant components of the pair potentials

Y. Tanuma,[1] Y. Tanaka,[2,3] and S. Kashiwaya[4]
[1]*Institute of Physics, Kanagawa University, Rokkakubashi, Yokohama, 221-8686, Japan*
[2]*Department of Applied Physics, Nagoya University, Nagoya, 464-8603, Japan*
[3]*CREST, Japan Science and Technology Cooperation (JST), Nagoya, 464-8603, Japan*
[4]*National Institute of Advanced Industrial Science and Technology, Tsukuba, 305-8568, Japan*
(Dated: February 2, 2008)

Superconducting proximity effect in normal metal (N) / $d_{x^2-y^2}$-wave superconductor (D) junctions in the presence of attractive interelectron potentials which can induce subdominant s-wave pair potentials both in N and D sides, is studied based on the quasiclassical Green's function theory, where spatial dependencies of the pair potentials are determined self-consistently. In the N/D junctions with orientational angle with $\theta = 0$, the s-wave component is induced in the N side by the proximity effect only for high transparent case, where the induced s-wave components in both the N and D sides do not break the time reversal symmetry (TRS). For fully transparent case, the resulting local density of states has a very sharp zero-energy peak (ZEP), the origin of which is the sign change of the pair potentials felt by the quasiparticles between the s-wave component in the N side and $d_{x^2-y^2}$-wave dominant component in the D side through Andreev reflections. On the other hands, for $\theta = \pi/4$, the subdominant s-wave component which breaks the TRS appears near the interface. Besides, for lower transparent cases, the subdominant imaginary s-wave component is also induced near the interface in the N side. The proximity induced s-wave component in the N side does not enhance the magnitude of the s-wave component of the pair potential which break the TRS in the D side. The resulting LDOS at the interface has the ZEP or its splitting depending on the transparency of the junction.

PACS numbers: 74.50.+r, 74.20.Rp, 74.72.-h

I. INTRODUCTION

To determine the pairing symmetry in unconventional superconductors is an interesting problem to understand the pairing mechanism of superconductivity. Nowadays, it is widely accepted that the superconducting pair potential of high-T_c cuprates has a $d_{x^2-y^2}$-wave symmetry in the bulk state.[1,2,3,4,5] In order to determine the pairing symmetry, several phase-sensitive probes have been used[1,2,4,5]. Among them tunneling spectroscopy via Andreev bound states (ABS's),[6,7,8,9,10,11,12,13,14,15,16] help us to detect the internal phase in the pair potential. The formation of ABS's at the Fermi energy (zero-energy), which is originated from the interference effect in the effective pair potential of $d_{x^2-y^2}$-wave symmetry through the reflection at the surface/interface, plays an important role when the angle θ between the lobe direction of the $d_{x^2-y^2}$-wave pair potential and the normal to the surface/interface is nonzero.[7] In fact, the existence of ABS's, which manifests itself as a distinct conductance peak at zero-bias in the tunneling spectrum (ZBCP), has been actually observed. Up to now, the consistency between theories[17,18,19,20,21,22,23,24,25,26,27,28,29,30,31,32,33,34] and experiments[35,36,37,38,39,40,41,42,43,44,45,46,47,48,49] has been checked in detail.

On the other hand, at the surface/interface of $d_{x^2-y^2}$-wave superconductor, it is known that the time-reversal symmetry (TRS) may be broken.[50,51,52] The reduction of the amplitude of $d_{x^2-y^2}$-wave pair potential near the surface/interface at low temperatures allows to induce the subdominant s-wave [d_{xy}-wave] component in the imaginary part of the pair potential, i.e., d+is-wave[11,18,19,20,53,54] [d+id'-wave[55,56,57]] state. The amplitude of the induced s-wave component has a maximum at $\theta = \pi/4$, which blocks the motion of quasiparticles. Then, the energy levels of ABS's shift from zero and the resulting tunneling spectra has a ZBCP splitting even in zero magnetic field. The observation of the ZBCP splitting without magnetic fields was believed to be one of the evidence for the broken time reversal symmetry states (BTRSS). However, actual tunneling experiments still remain to be controversial. In fact, some groups[39,40,43,44,45,46] have reported the ZBCP splitting and they ascribed the origin of the ZBCP splitting to the above BTRSS. At the same time, there are other experiments which do not show the ZBCP splitting, and in these experiments, the ZBCP survives even at low temperature.[37,38,41,42,47,48,49] Moreover, a critical current measurement of grain boundary junctions in high-T_c cuprates concluded the absence of BTRSS at the interface.[58] It has been studied in detail that the ZBCP splitting in the tunneling spectra is sensitive to several factors: (i) transmission probability of the junctions,[59] (ii) roughness at the interface,[17,18,19] and (iii) effect of impurity scattering in normal metals or superconductors.[23,25] Recent studies by Asano *et al.*,[23] revealed that the existence of the impurity scattering can induce the ZBCP splitting even without BTRSS. Taking account of these situations, one can not conclude that the observation of the ZBCP splitting by tunneling experiments directly indicate the presence of the BTRSS

near the surface/interface.

More recently, it is proposed that the induced s-wave component of the pair potential by proximity effect in normal metals (N) may enhance the magnitude of the subdominant s-wave component in $d_{x^2-y^2}$-wave superconductors (D), which forms the BTRSS based on the analysis of the tunneling experiments.[60] It is of great interest to study whether the induced s-wave component in the N side by the proximity effect has the influence on the subdominant component in the D side which forms the BTRSS. The proximity effect in the N/D junction without the BTRSS was theoretically studied by Ohashi.[61] It is shown that the amplitude of the subdominant is-wave is the largest at $\theta = \pi/4$. For $\theta = 0$ with fully transparent junctions, local density of states (LDOS) at the interface has a zero energy peak (ZEP), the origin of which is not ABS but the sign change of the pair potentials between N and D sides felt by Andreev reflection of quasiparticles. It is necessary to study the interplay between the proximity effect and the BTRSS by changing the orientational angle θ. At the same time, it is also interesting to clarify the relationship between the different origin of two kinds of ZEP's. One is the ZEP which originates from the formation of ABS for $\theta \neq 0$. The other is due to the proximity effect expected for fully transparent junctions for $\theta = 0$.[61]

In the present paper, we study the proximity effect in N/D junctions on the basis of quasiclassical Green's function methods. We assume attractive interelectron potentials which induce subdominant s-wave components in the N side as well as the D. The spatial dependencies of the pair potentials both in the N and D sides are determined self-consistently. The LDOS at the interface of the N/D junctions are studied in detail by changing θ and the transparency of the junction. For $\theta = \pi/4$, the magnitude of the s-wave component is induced even in the N side, while the subdominant s-wave component which breaks TRS exists near the interface on the D side.[62] On the other hand, for $\theta = 0$, s-wave component is induced in the N side by the proximity effect with the increase of the transparency of the junction. The induced s-wave component in the N side and that in the D side do not break the TRS. It is revealed that the proximity induced s-wave component in the N side does not enhance the BTRSS in the D side.

The organization of the present paper is as follows. In Sec. II, a theoretical formulation to calculate the spatial dependence of the pair potential, and local density of states is presented. In Sec. III, results of the numerical calculations are discussed in detail. Finally, we summarize the paper in Sec. IV.

II. THEORETICAL MODEL

In the present paper, we consider the N/D junction separated by an insulating interface at $x = 0$, where the normal metal is located at $x < 0$ and the $d_{x^2-y^2}$-wave superconductor extends elsewhere (Fig. 1). For the simplicity, two dimensional system is assumed and the x axis is taken perpendicular to the interface. When quasiparticles are in the xy plane, a transmitted electron like quasiparticle and holelike quasiparticle in the D side feel different effective pair potentials $\Delta_d(\phi_+)$ and $\Delta_d(\phi_-)$, with $\phi_+ = \phi$ and $\phi_- = \pi - \phi$. Here ϕ is the azimuthal angle in the xy plane given by $(k_x + \mathrm{i}k_y)/|\boldsymbol{k}| = \mathrm{e}^{\mathrm{i}\phi}$. Besides, a cylindrical Fermi surface is assumed and the magnitude of the Fermi momentum and the effective mass are chosen to be equal both in the N and D sides.

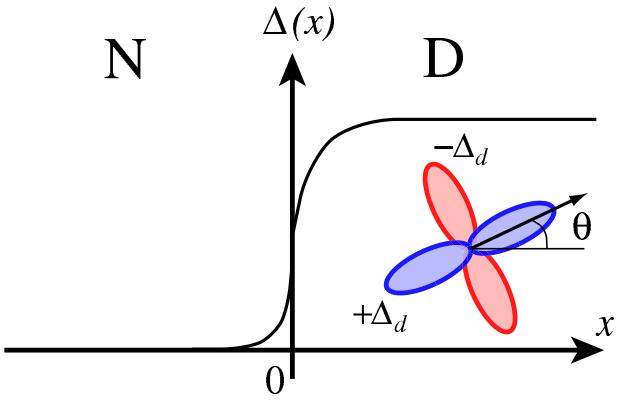

FIG. 1: Schematic illustration of a N/D junction with a spatially varying pair potential. The misorientation angle θ denotes the angle between the crystal axis of $d_{x^2-y^2}$-wave superconductor and the normal to the interface.

In order to study the proximity effect in the N/D junction, we determine the spatial variation of the pair potentials self-consistently. For this purpose, we make use of the quasi-classical Green's function procedure[63] developed by Nagai and co-workers.[64,65] In the following, we briefly summarize this scheme we employed. We introduce the generalized Eilenberger equation,[63]

$$\mathrm{i}|v_{\mathrm{F}x}|\frac{\partial}{\partial x}g_{\alpha\beta}(\phi,x) = -\alpha\left[\mathrm{i}\omega_m\hat{\tau}_3 + \hat{\Delta}(\phi_\alpha,x)\right]g_{\alpha\beta}(\phi,x) + \beta g_{\alpha\beta}(\phi,x)\left[\mathrm{i}\omega_m\hat{\tau}_3 + \hat{\Delta}(\phi_\beta,x)\right], \tag{1}$$

$$\hat{\Delta}(\phi_\alpha,x) = \begin{pmatrix} 0 & \Delta(\phi_\alpha,x) \\ -\Delta(\phi_\alpha,x)^* & 0 \end{pmatrix}, \tag{2}$$

where $v_{\mathrm{F}x} = v_{\mathrm{F}}\cos\theta$ and $\hat{\tau}_i (i = 1,2,3)$ stand for the x component of the Fermi velocity and the Pauli matrices, respectively. Here $\omega_m = \pi T(2m+1)$ (m: integer) is the Matsubara frequency.

Now, considering a semi-infinite N/D junction geometry, the pair potential in D [N] side tend to the bulk value [zero] $\Delta^{\mathrm{D}}(\phi_\alpha,\infty)$ [$\Delta^{\mathrm{N}}(\phi_\alpha,-\infty)$] at sufficiently large x. In semi-infinite limit, we can find the quasi-classical Green's function $\hat{g}^l_{\alpha\alpha}(\phi_\alpha,x)$ for $l(=\mathrm{N,D})$ regions given by[61,64,66]

$$\hat{g}^l_{\alpha\alpha}(\phi_\alpha,x) = \mathrm{i}\left(\frac{2\hat{A}^l_\alpha(x)}{\mathrm{Tr}[\hat{A}^l_\alpha(x)]} - \mathbf{1}\right), \tag{3}$$

Following equations are satisfied for the N side,

$$\hat{A}^{\rm N}_{+}(x) = \tilde{U}^{\rm N}_{+}(\phi_+, x, 0)\hat{R}_{\rm D}\hat{\lambda}^{\rm N}(0, x), \tag{4}$$

$$\hat{A}^{\rm N}_{-}(x) = \hat{\lambda}^{\rm N}(x, 0)\hat{R}_{\rm D}\tilde{U}^{\rm N}_{-}(\phi_-, 0, x), \tag{5}$$

$$\hat{\lambda}^{\rm N}(x, x') = \begin{pmatrix} 1 & {\rm i}/\mathcal{G}^{\rm N}_{+}(x') \\ {\rm i}\mathcal{G}^{\rm N}_{-}(x) & -\mathcal{G}^{\rm N}_{-}(x)/\mathcal{G}^{\rm N}_{+}(x') \end{pmatrix},$$

and for the D side,

$$\hat{A}^{\rm D}_{+}(x) = \hat{\lambda}^{\rm D}(x, 0)\hat{R}_{\rm N}\tilde{U}^{\rm D}_{+}(\phi_+, 0, x), \tag{6}$$

$$\hat{A}^{\rm D}_{-}(x) = \tilde{U}^{\rm D}_{-}(\phi_-, x, 0)\hat{R}_{\rm N}\hat{\lambda}^{\rm D}(0, x), \tag{7}$$

$$\hat{\lambda}^{\rm D}(x, x') = \begin{pmatrix} 1 & {\rm i}/\mathcal{G}^{\rm D}_{-}(x') \\ {\rm i}\mathcal{G}^{\rm D}_{+}(x) & -\mathcal{G}^{\rm D}_{+}(x)/\mathcal{G}^{\rm D}_{-}(x') \end{pmatrix},$$

respectively. In the above, $\hat{R}_{\rm N}$ and $\hat{R}_{\rm D}$ are matrices with reflection probability R at the interface given by[61]

$$\hat{R}_{\rm N} \propto \begin{pmatrix} \mathcal{G}^{\rm N}_{+}(0) - R\mathcal{G}^{\rm N}_{-}(0) & {\rm i}(1-R) \\ {\rm i}(1-R)\mathcal{G}^{\rm N}_{-}(0)\mathcal{G}^{\rm N}_{+}(0) & \mathcal{G}^{\rm N}_{+}(0)R - \mathcal{G}^{\rm N}_{-}(0) \end{pmatrix}, \tag{8}$$

$$\hat{R}_{\rm D} \propto \begin{pmatrix} \mathcal{G}^{\rm D}_{-}(0) - R\mathcal{G}^{\rm D}_{+}(0) & {\rm i}(1-R) \\ {\rm i}(1-R)\mathcal{G}^{\rm D}_{+}(0)\mathcal{G}^{\rm D}_{-}(0) & \mathcal{G}^{\rm D}_{-}(0)R - \mathcal{G}^{\rm D}_{+}(0) \end{pmatrix}. \tag{9}$$

Here, we define $\mathcal{G}^{l}_{\alpha}(x)$ given by

$$\mathcal{G}^{\rm N}_{\alpha}(x) = -{\rm i}\frac{v^{\rm N(+)}_n(\phi_\alpha, x)}{u^{\rm N(+)}_n(\phi_\alpha, x)}, \quad \mathcal{G}^{\rm D}_{\alpha}(x) = -{\rm i}\frac{v^{\rm D(-)}_n(\phi_\alpha, x)}{u^{\rm D(-)}_n(\phi_\alpha, x)}. \tag{10}$$

Next, in order to obtain the quantities $\tilde{U}^{l}_{\alpha}(\phi_\alpha, x, x')$ in Eqs. (4)-(7), we rewrite $\hat{A}^{l}_{\alpha}(x)$ as[64,66]

$$\hat{A}^{\rm N}_{+}(x) = \begin{pmatrix} X^{\rm N}_{+}(x) \\ Y^{\rm N}_{+}(x) \end{pmatrix} \begin{pmatrix} u^{\rm N(+)}_n(\phi_+, x) & v^{\rm N(+)}_n(\phi_+, x) \end{pmatrix} \hat{\tau}_2, \tag{11}$$

$$\hat{A}^{\rm N}_{-}(x) = \begin{pmatrix} u^{\rm N(+)}_n(\phi_-, x) \\ v^{\rm N(+)}_n(\phi_-, x) \end{pmatrix} \begin{pmatrix} X^{\rm N}_{-}(x) & Y^{\rm N}_{-}(x) \end{pmatrix} \hat{\tau}_2, \tag{12}$$

$$\hat{A}^{\rm D}_{+}(x) = \begin{pmatrix} u^{\rm D(-)}_n(\phi_+, x) \\ v^{\rm D(-)}_n(\phi_+, x) \end{pmatrix} \begin{pmatrix} X^{\rm D}_{+}(x) & Y^{\rm D}_{+}(x) \end{pmatrix} \hat{\tau}_2, \tag{13}$$

$$\hat{A}^{\rm D}_{-}(x) = \begin{pmatrix} X^{\rm D}_{-}(x) \\ Y^{\rm D}_{-}(x) \end{pmatrix} \begin{pmatrix} u^{\rm D(-)}_n(\phi_-, x) & v^{\rm D(-)}_n(\phi_-, x) \end{pmatrix} \hat{\tau}_2, \tag{14}$$

with

$$\begin{pmatrix} X^{\rm N}_{-}(x) \\ Y^{\rm N}_{-}(x) \end{pmatrix} = \tilde{U}^{\rm N}_{+}(\phi_+, x, 0)\hat{R}_{\rm D} \begin{pmatrix} u^{\rm N(+)}_n(\phi_-, 0) \\ v^{\rm N(+)}_n(\phi_-, 0) \end{pmatrix}, \tag{15}$$

$$\begin{pmatrix} X^{\rm N}_{-}(x) & Y^{\rm N}_{-}(x) \end{pmatrix} \hat{\tau}_2 = \begin{pmatrix} u^{\rm N(+)}_n(\phi_+, 0) & v^{\rm N(+)}_n(\phi_+, 0) \end{pmatrix} \hat{\tau}_2 \times \hat{R}_{\rm D}\tilde{U}^{\rm N}_{-}(\phi_-, 0, x), \tag{16}$$

$$\begin{pmatrix} X^{\rm D}_{+}(x) & Y^{\rm D}_{+}(x) \end{pmatrix} \hat{\tau}_2 = \begin{pmatrix} u^{\rm D(-)}_n(\phi_-, 0) & v^{\rm D(-)}_n(\phi_-, 0) \end{pmatrix} \hat{\tau}_2 \times \hat{R}_{\rm N}\tilde{U}^{\rm D}_{+}(\phi_+, 0, x), \tag{17}$$

$$\begin{pmatrix} X^{\rm D}_{-}(x) \\ Y^{\rm D}_{-}(x) \end{pmatrix} = \tilde{U}^{\rm D}_{-}(\phi_-, x, 0)\hat{R}_{\rm N} \begin{pmatrix} u^{\rm D(-)}_n(\phi_+, 0) \\ v^{\rm D(-)}_n(\phi_+, 0) \end{pmatrix}. \tag{18}$$

Then we define $\mathcal{F}^{l}_{\alpha}(x)$ given by

$$\mathcal{F}^{\rm N}_{\alpha}(x) = {\rm i}\frac{X^{\rm N}_{\alpha}(x)}{Y^{\rm N}_{\alpha}(x)}, \quad \mathcal{F}^{\rm D}_{\alpha}(x) = {\rm i}\frac{X^{\rm D}_{\alpha}(x)}{Y^{\rm D}_{\alpha}(x)}. \tag{19}$$

Here, $\mathcal{G}^{l}_{\alpha}(x)$ and $\mathcal{F}^{l}_{\alpha}(x)$ in Eqs. (10) and (19), obey the following Riccati type equations:

$$\hbar|v_{{\rm F}x}|\frac{\partial}{\partial x}\mathcal{G}^{l}_{\alpha}(x) = \alpha\left[2\omega_m\mathcal{G}^{l}_{\alpha}(x) + \Delta^{l}(\phi_\alpha, x)\mathcal{G}^{l}_{\alpha}(x)^2 - \Delta^{l}(\phi_\alpha, x)^*\right], \tag{20}$$

$$\hbar|v_{{\rm F}x}|\frac{\partial}{\partial x}\mathcal{F}^{l}_{\alpha}(x) = -\alpha\left[2\omega_m\mathcal{F}^{l}_{\alpha}(x) - \Delta^{l}(\phi_\alpha, x)^*\mathcal{F}^{l}_{\alpha}(x)^2 + \Delta^{l}(\phi_\alpha, x)\right]. \tag{21}$$

We can write the quasi-classical Green's function in a compact form[64]

$$\hat{g}^{\rm N}_{--}(\phi_-, x) = \frac{\rm i}{1 - \mathcal{G}^{\rm N}_{-}(x)\mathcal{F}^{\rm N}_{-}(x)} \begin{pmatrix} 1 + \mathcal{G}^{\rm N}_{-}(x)\mathcal{F}^{\rm N}_{-}(x) & 2{\rm i}\mathcal{F}^{\rm N}_{-}(x) \\ 2{\rm i}\mathcal{G}^{\rm N}_{-}(x) & -1 - \mathcal{G}^{\rm N}_{-}(x)\mathcal{F}^{\rm N}_{-}(x) \end{pmatrix}, \tag{22}$$

$$\hat{g}^{\rm D}_{++}(\phi_+, x) = \frac{\rm i}{\mathcal{G}^{\rm D}_{+}(x)\mathcal{F}^{\rm D}_{+}(x) - 1} \begin{pmatrix} \mathcal{G}^{\rm D}_{+}(x)\mathcal{F}^{\rm D}_{+}(x) + 1 & 2{\rm i}\mathcal{F}^{\rm D}_{+}(x) \\ 2{\rm i}\mathcal{G}^{\rm D}_{+}(x) & -\mathcal{G}^{\rm D}_{+}(x)\mathcal{F}^{\rm D}_{+}(x) - 1 \end{pmatrix}, \tag{23}$$

with $\hat{g}^{l}_{--}(\phi_-, x) = -\hat{g}^{l}_{++}(-\phi_+, x)^\dagger$. Initial conditions of these equations are as follows,

$$\mathcal{G}^{\rm N}_{-}(-\infty) = 0, \quad \mathcal{G}^{\rm D}_{\alpha}(\infty) = \frac{\Delta^{\rm D}(\phi_\alpha, \infty)^*}{\omega_m + \alpha\Omega^{\rm D}_{\alpha}}, \tag{24}$$

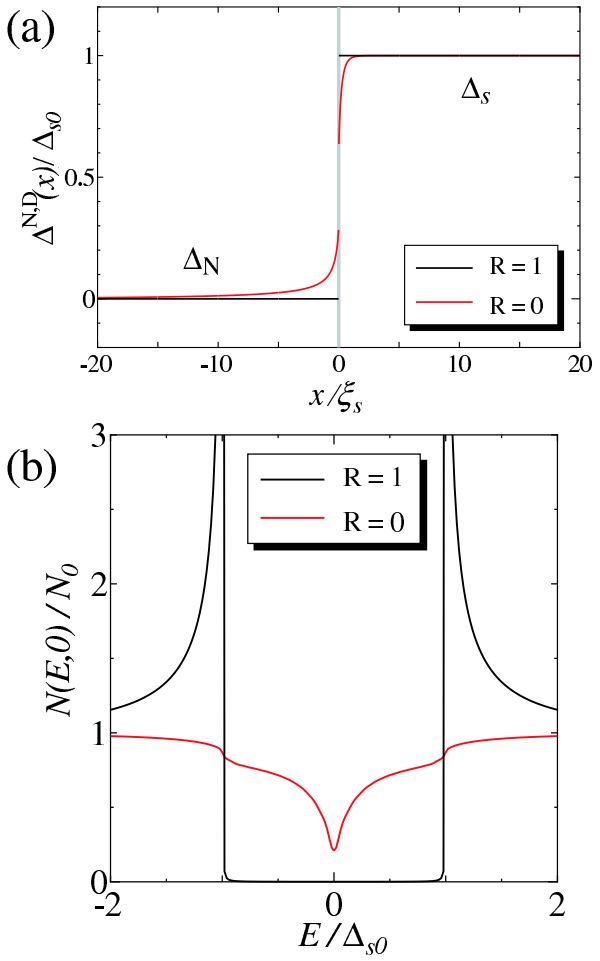

FIG. 2: (a) Spatial dependence of the pair potentials in a normal metal /s-wave superconductor (N/S) junction with $T = 0.02T_s$ and $T_N/T_s = 10^{-3}$. (b) The corresponding local density of states (LDOS) at the S side of the interface.

with $\Omega_\alpha^l = \sqrt{\omega_m^2 + |\Delta^l(\phi_\alpha, \infty)|^2}$. Moreover, the boundary condition of the $\mathcal{G}_\alpha^l(0)$ and $\mathcal{F}_\alpha^l(0)$ at the interface $x = 0$ are

$$\mathcal{F}_+^{\rm N} = \frac{\mathcal{G}_-^{\rm D} - R\mathcal{G}_+^{\rm D} - (1-R)\mathcal{G}_-^{\rm N}}{[R\mathcal{G}_-^{\rm D} - \mathcal{G}_+^{\rm D}]\mathcal{G}_-^{\rm N} + (1-R)\mathcal{G}_+^{\rm D}\mathcal{G}_-^{\rm D}}, \quad (25)$$

$$\mathcal{F}_-^{\rm N} = \frac{R\mathcal{G}_-^{\rm D} - \mathcal{G}_+^{\rm D} + (1-R)\mathcal{G}_+^{\rm N}}{\mathcal{G}_+^{\rm N}[\mathcal{G}_-^{\rm D} - R\mathcal{G}_+^{\rm D}] - (1-R)\mathcal{G}_-^{\rm D}\mathcal{G}_+^{\rm D}}, \quad (26)$$

$$\mathcal{F}_+^{\rm D} = \frac{R\mathcal{G}_+^{\rm N} - \mathcal{G}_-^{\rm N} + (1-R)\mathcal{G}_-^{\rm D}}{\mathcal{G}_-^{\rm D}[\mathcal{G}_+^{\rm N} - R\mathcal{G}_-^{\rm N}] - (1-R)\mathcal{G}_+^{\rm N}\mathcal{G}_-^{\rm N}}, \quad (27)$$

$$\mathcal{F}_-^{\rm D} = \frac{\mathcal{G}_+^{\rm N} - R\mathcal{G}_-^{\rm N} - (1-R)\mathcal{G}_+^{\rm D}}{[R\mathcal{G}_+^{\rm N} - \mathcal{G}_-^{\rm N}]\mathcal{G}_+^{\rm D} + (1-R)\mathcal{G}_-^{\rm N}\mathcal{G}_+^{\rm N}}. \quad (28)$$

The pair potentials for both N and D sides are given by[53,61,65,66,67]

$$\Delta^l(\phi, x) = \sum_{0\le m<\omega_c/2\pi T} \frac{1}{2\pi}\int_{-\pi/2}^{\pi/2} d\phi' \sum_\alpha V^l(\phi, \phi'_\alpha) \times [\hat{g}^l_{\alpha\alpha}(\phi'_\alpha, x)]_{12}, \quad (29)$$

where ω_c is the cutoff energy and $[\hat{g}^l_{\alpha\alpha}(\phi_\alpha, x)]_{12}$ means the 12 element of $\hat{g}^l_{\alpha\alpha}(\phi_\alpha, x)$. Here $V^l(\phi, \phi_\alpha)$ is the effective inter-electron potential of the Cooper pair in the l side. In our numerical calculations, new $\Delta^l(\phi_\alpha, x)$ and $\hat{g}^l_{\alpha\alpha}(\phi_\alpha, x)$ are obtained using Eqs.(20)-(23) and (29). We reiterate this process until the convergence is sufficiently obtained.

Based on the self-consistently determined pair potentials, the LDOS can be calculated as,

$$N_l(E, x) = \frac{1}{\pi}\int_{-\pi/2}^{\pi/2} d\phi n_l(E, \phi, x), \quad (30)$$

$$n_l(E, \phi, x) = {\rm Im}\left\{\frac{N_0}{2}{\rm Tr}\left[\hat{g}^l_{\alpha\alpha}(\phi_\alpha, x)\hat{\tau}_3\right]\right\}_{i\omega_m \to E+i\delta}, \quad (31)$$

where N_0 means the density of states (DOS) in normal states, and δ is infinitesimal. In this paper, we choose the temperature T as $T/T_d = 0.02$, where T_d is the critical temperature of the bulk $d_{x^2-y^2}$-wave superconductor.

III. RESULTS OF NUMERICAL CALCULATIONS

In this section, we show our results of numerical calculations on the spatial dependence of the self-consistently determined pair potentials and the corresponding LDOS. The spatial variation of the pair potentials in the N/D junction is expressed as

$$\Delta^{\rm N}(\phi, x) = \Delta_{\rm N}(x), \quad (32)$$

$$\Delta^{\rm D}(\phi, x) = \Delta_d(x)\cos 2(\phi - \theta) + \Delta_s(x), \quad (33)$$

where $\Delta_{\rm N}(x)$, $\Delta_d(x)$, and $\Delta_s(x)$ denote the amplitude of s-wave component in the N side, $d_{x^2-y^2}$-wave component in the D side, and subdominant s-wave component in the D side, respectively. The attractive potentials $V^l(\phi, \phi')$ with $l = {\rm N}, {\rm D}$, are given by

$$V^{\rm N}(\phi, \phi') = V_{\rm N}, \quad (34)$$

$$V^{\rm D}(\phi, \phi') = 2V_d\cos(2\phi - 2\theta)\cos(2\phi' - 2\theta) + V_s, \quad (35)$$

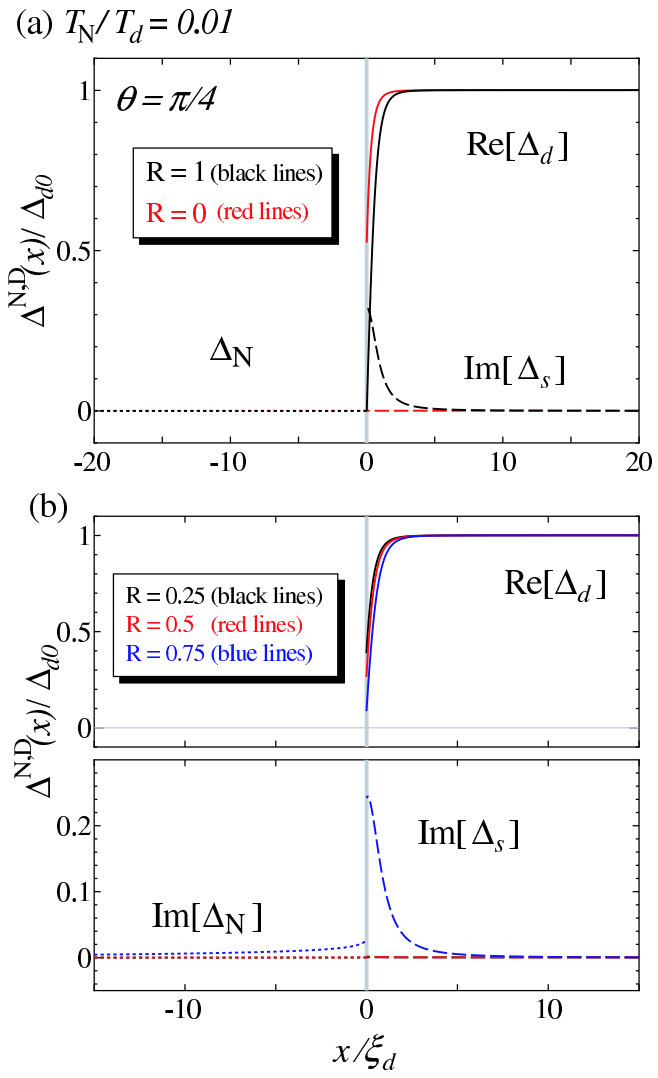

FIG. 3: Spatial dependence of the pair potentials in N/D junctions with $\theta = \pi/4$ and $T_N/T_d = 0.01$. (a) $R = 0$ and 1, (b) $R = 0.25$, 0.5, and 0.75.

and

$$V_N = \frac{2\pi k_B T}{\ln\frac{T}{T_N} + \sum_{0\le m<\omega_c/2\pi T}\frac{1}{m+1/2}}, \quad (36)$$

$$V_d = \frac{2\pi k_B T}{\ln\frac{T}{T_d} + \sum_{0\le m<\omega_c/2\pi T}\frac{1}{m+1/2}}, \quad (37)$$

$$V_s = \frac{2\pi k_B T}{\ln\frac{T}{T_s} + \sum_{0\le m<\omega_c/2\pi T}\frac{1}{m+1/2}}. \quad (38)$$

Here, T_N denotes the transition temperature of s-wave pair potential in the N side. T_s denotes the transition temperature of s-wave pair potential in the D side without $d_{x^2-y^2}$-wave attractive potential.

First, in order to understand the role of the proximity effect clearly, let us check the case of normal metal/s-wave superconductor (N/S) junctions. Figure 2(a) shows the obtained spatial dependence of the pair potentials in the junctions for extremely low ($R = 1$) and high ($R = 0$) transparency cases. The x-axis of Fig. 2 is normalized by $\xi_s = \hbar v_F/\pi\Delta_{s0}$, which is the coherence length of s-wave superconductor. For $R = 1$, the s-wave pair potential remains to be constant in S side, whereas the pair potential in the N side is zero. The spatial variation of the pair potentials is represented as a step function. The resulting LDOS at the interface reproduces the bulk U-shaped DOS [see Fig. 2(b)]. On the other hands, for $R = 0$, the pair potential Δ_N in the N side survives toward the inside. We can see that the LDOS at the interface in the presence of the proximity effect is different from the bulk DOS.

A. N/D junction with $\theta = \pi/4$

In this subsection, we focus on the N/D junction with (110)-oriented interface ($\theta = \pi/4$). As the parameter of the subdominant s-wave component, we take $T_s/T_d = 0.3$ in the following. In Figs. 3(a) and 3(b), the spatial variations of the pair potentials is shown for $T_N/T_d = 0.01$ for $R = 0$, 1, and 0.25, 0.5, 0.75, respectively. Here, Re[$\Delta_d(x)$] and Im[$\Delta_{N,s}(x)$] denote real part of $\Delta_d(x)$ and imaginary part of $\Delta_{N,s}(x)$, respectively. The x-axis of Fig. 3 is normalized by the $d_{x^2-y^2}$-wave coherence length $\xi_d = \hbar v_F/\pi\Delta_{d0}$, where Δ_{d0} is $d_{x^2-y^2}$-wave pair potential in bulk states.

First, we present our results in the light of previous theories.[7,53,69] The reduction of Re[$\Delta_d(x)$] originates from a depairing effect that the effective pair potentials $\Delta^D(\phi_+, 0)$ and $\Delta^D(\phi_-, 0)$ have reversed contribution to the pairing interaction for certain range of ϕ. Re[$\Delta_d(x)$] is suppressed at the interface in the D side. At the same time, the quasiparticle forms the ABS with zero-energy at the interface.[7,69] When the magnitude of the reflection probability R approaches unity, the ABS becomes unstable with the introduction of the subdominant s-wave attractive potential in the D side. And then Im[$\Delta_s(x)$] is induced in the vicinity of the interface in the D side in low transparent cases with large magnitude of R.[53] As regards the proximity effect in the N side, the pair potential $\Delta_N(x)$ is not induced for fully high and low transparent cases. However, the imaginary component of $\Delta_N(x)$ is enhanced nearly in $R = 0.75$ [see Fig. 3]. We can recognize that the existence of Im[$\Delta_s(x)$] near the interface of D side can allow the enhancement of the Im[$\Delta_N(x)$]. This fact is more recently found by Löfwander,[62] and our results are consistent with his work.

In Figs. 4(a) and 4(b), we show the corresponding LDOS at the D side of the interface, where the same parameters of Figs. 3(a) and 3(b) are used, respectively. For $R = 0$, $N_D(E, 0)$ is equal to N_0 and has no E dependence. If we neglect the induced s-wave component in the N

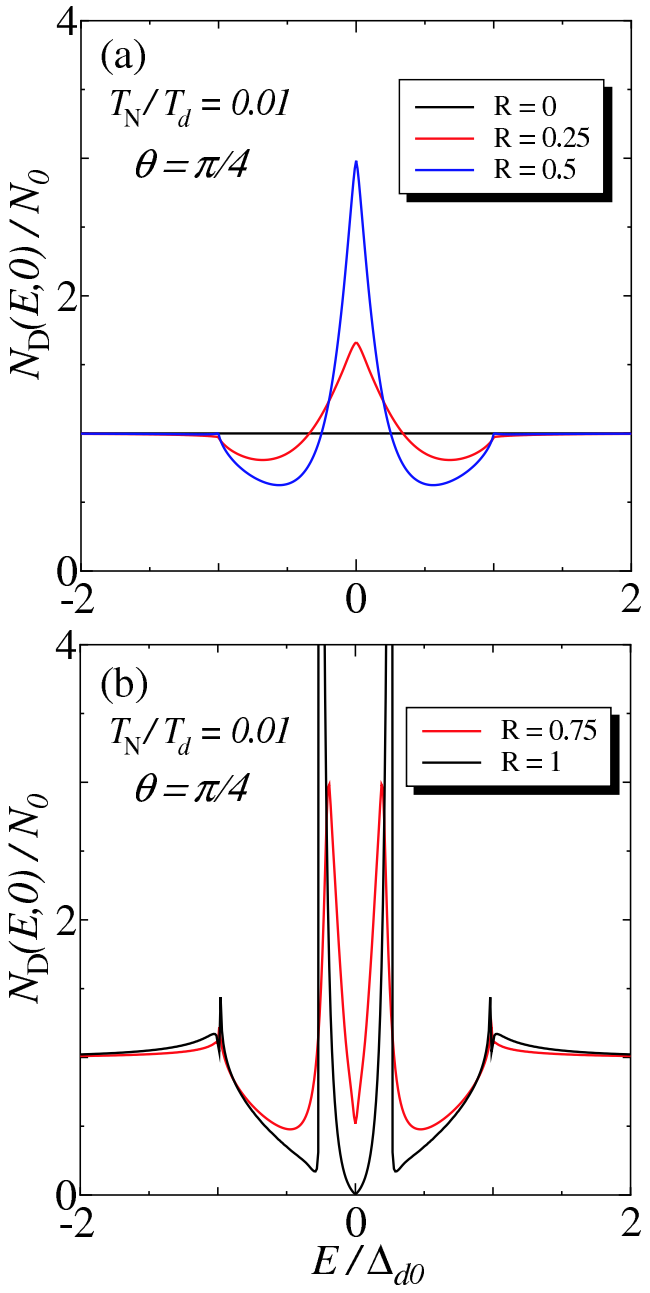

FIG. 4: The LDOS for the N/D junction with $\theta = \pi/4$ and $T_N/T_d = 0.01$. (a) $R = 0$, 0.25, and 0.5, (b) $R = 0.75$ and 1.

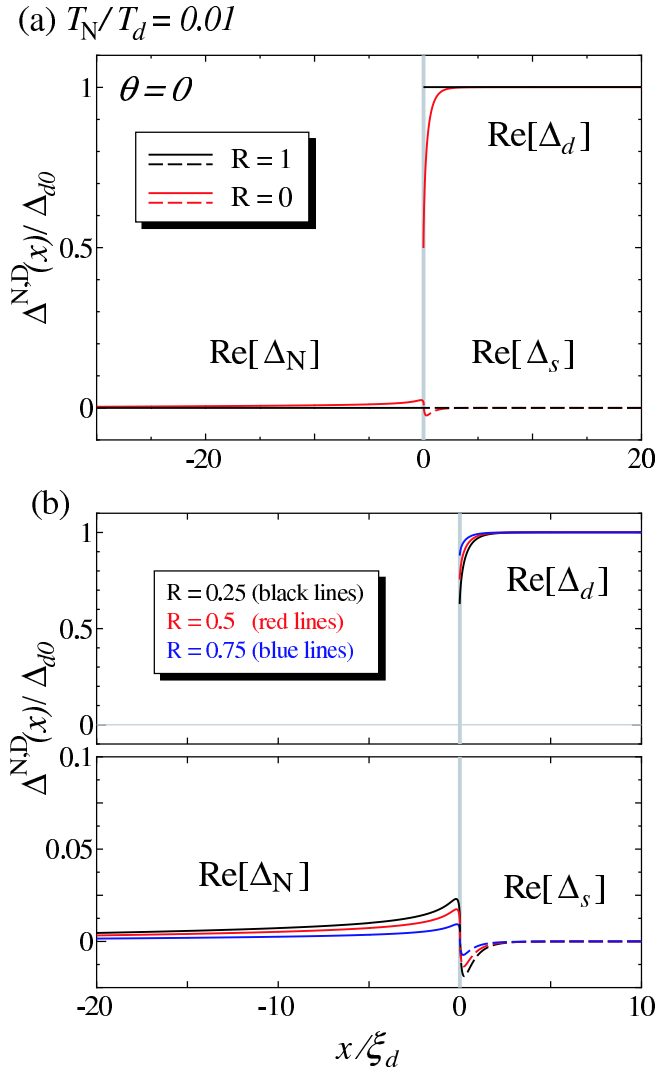

FIG. 5: Spatial dependencies of the pair potentials in N/D junctions with $\theta = 0$ and $T_N/T_d = 0.01$. (a) $R = 0$ and 1, (b) $R = 0.25$, 0.5, and 0.75.

side, the resulting LDOS has a zero-energy enhanced line shapes for small R.[59] This is because that the magnitude of the subdominant s-wave component, *i.e.*, $\mathrm{Im}[\Delta_s(x)]$ is very small and the incident and reflected quasiparticles normal to the interface can feel opposite signs of the $d_{x^2-y^2}$-wave pair potentials. However, as shown in Fig. 3(b), not only $\mathrm{Im}[\Delta_N(x)]$ but also $\mathrm{Im}[\Delta_s(x)]$ remain to be non-zero due to the proximity effect. In this case, the resulting LDOS has complex line shapes. For $R = 1$, due to the enhancement of the magnitude of $\mathrm{Im}[\Delta_s(x)]$, the LDOS has the ZEP splitting, which is consistent with the previous works[11,53,59].

B. N/D junction with $\theta = 0$

In this subsection, we focus on the N/D junction with $\theta = 0$ and $T_N/T_d = 0.01$. The spatial dependencies of the pair potentials $\mathrm{Re}[\Delta_N(x)]$, $\mathrm{Re}[\Delta_d(x)]$, and $\mathrm{Re}[\Delta_s(x)]$, are plotted in Figs. 5(a) and 5(b), for $R = 0$, 1, and 0.25, 0.5, 0.75, respectively. For the low transparent limit, $R = 1$, [see Fig. 5(a)], the amplitude of the pair potential is constant. This situation is similar to the case of the N/S junctions with $R = 1$ [see Fig. 2(a)]. With the decrease of R, $\mathrm{Re}[\Delta_d(x)]$ is suppressed near the interface, while $\mathrm{Re}[\Delta_s(x)]$ is slightly mixed in the vicinity of the interface. Since $\mathrm{Im}[\Delta_s(x)] = 0$ is satisfied, the TRS is not broken near the (100) interface. On the other hand for the N

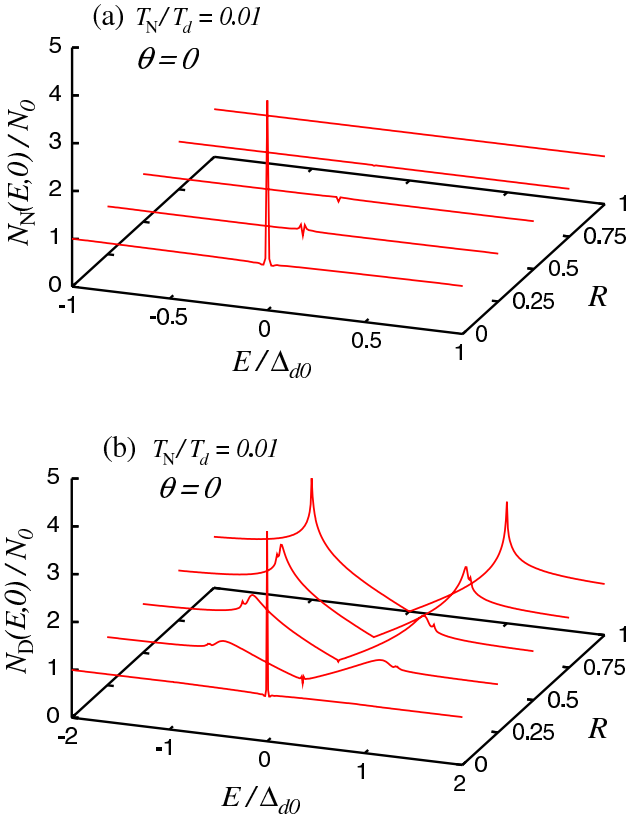

FIG. 6: (a) The LDOS at the interface by its value in the normal state for various R with $\theta = 0$ and $T_N/T_d = 0.01$. (a) The N side, and (b) the D side.

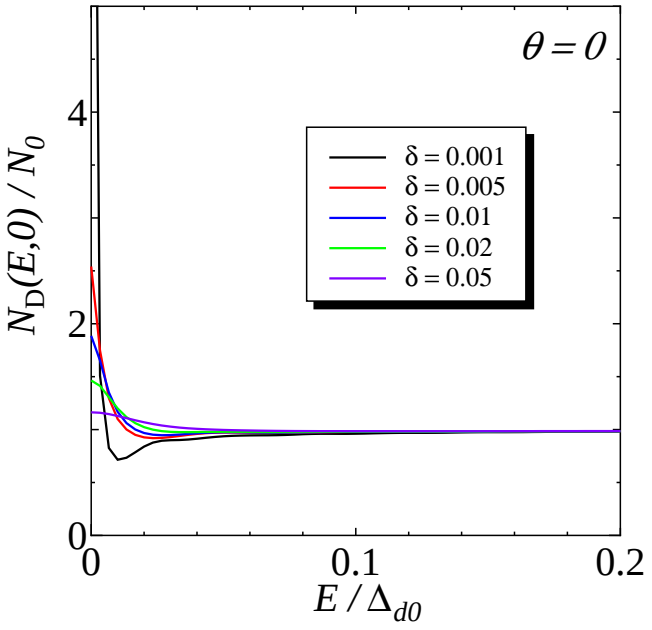

FIG. 7: The LDOS at the interface near zero energy with $R = 0$ for various δ.

side, we can readily see that the pair potential $\mathrm{Re}[\Delta_N(x)]$ is induced. This indicates that the superconducting pair potential penetrates into the N side due to the proximity effect.[61] With increasing the magnitude of T_N, the amplitude of $\mathrm{Re}[\Delta_N(x)]$ becomes larger. However, both $\mathrm{Im}[\Delta_s(x)] = 0$ and $\mathrm{Im}[\Delta_N(x)] = 0$ are satisfied. This situation is significantly different from the corresponding case of $\theta = \pi/4$ where the TRS is broken.

Next, let us look at the corresponding LDOS at the interface. We show that the LDOS at the interface in the N and D sides as shown in Fig. 6. For $R = 1$, the LDOS on the D side has a V-shaped structure similar to the bulk d-wave density of states.[11,53,59] The corresponding LDOS in the N side is constant. With the decrease of the magnitude of R, the magnitude of LDOS in the D side around zero energy is enhanced while that around $\pm\Delta_{d0}$ is suppressed. For $R = 0.25$, the LDOS has a small dip like structure both in the N and D sides. The fine structure around zero energy is due to the induced pair potential $\Delta_N(x)$ in the N side. The extreme case is $R = 0$, where normal reflection is absent. The pair potential $\mathrm{Re}[\Delta_N(x)]$ induces the ZEP in the LDOS [see Fig. 6] through Andreev reflection.[61]

Now we concentrate on the width of this ZEP. We see that the relevance of the peak width and the infinitesimal number δ introduced in Eq.(31) in order to avoid divergence in the actual calculation where the inverse of δ can be regarded as a life time of quasiparticles. As shown in Fig. 7, the width of the ZEP becomes narrow with the decrease of the magnitude of δ, while the height of it increases monotonically. For $\delta \to 0$ limit, the ZEP is reduced to be expressed by the δ-function.

In Fig. 8, we show the spatial dependence of LDOS in the N side ($x < 0$). For $R = 0$, the zero energy states formed at the interface penetrate into the N side. The width and the height of the ZEP is reduced with the increase of the magnitude of x. For $R = 0.1$, the LDOS has a mini gap. The width of the gap has a spatial dependence since the induced pair potential $\mathrm{Re}[\Delta_N(x)]$ depends on x. The width of the mini gap is reduced with the increase of the magnitude of x.

At the end of this subsection, let us remark on the difference on the origin of ABS's between $\theta = \pi/4$ and $\theta = 0$. As mentioned in Sec. III A, the formation of ABS's is originated from the opposite sign of the pair potentials between $\Delta_d(\phi_+, 0)$ and $\Delta_d(\phi_-, 0)$ felt by quasiparticles in the D side. However, in the case of $\theta = 0$, there is no sign change between $\Delta_d(\phi_+, 0)$ and $\Delta_d(\phi_-, 0)$ for any ϕ. This manifestation of the ZEP in the LDOS is due to the another origin. It is due to the sign change of the pair potentials between $\mathrm{Re}[\Delta_N(x)]$ and $\mathrm{Re}[\Delta_s(x)]$ or that between $\mathrm{Re}[\Delta_N(x)]$ and $\mathrm{Re}[\Delta_d(x)]$ for $|\phi| > \pi/4$ through the Andreev reflection. Actually, by calculating the angle resolved LDOS $n_D(E, \phi, x)$ in Eq.(31), $n_D(E, \phi, x)$ has the ZEP for $\phi = \pi/3$ while it does not for $\phi = \pi/6$ as shown in Fig. 9.

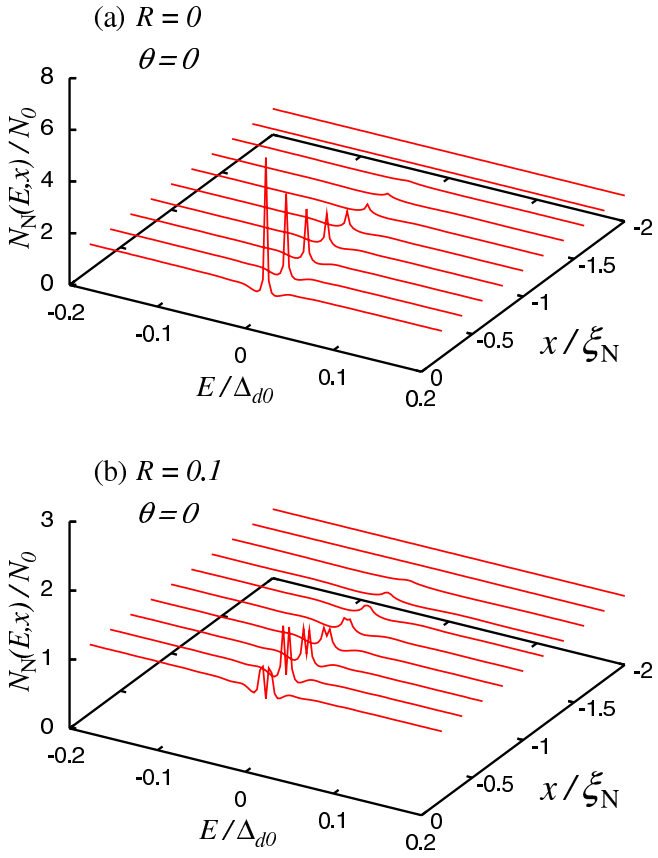

FIG. 8: The LDOS at $x < 0$ with $\theta = 0$. (a) $R = 0$ and (b) $R = 0.1$ for various x. Here $\xi_{\rm N} = v_{\rm F}/2\pi T$ is the coherence length in the N side with $T = 0.02T_d$.

C. N/D junction with $\theta = \pi/6$

In this subsection, we concentrate on the case with intermediate angle θ, *e.g.*, $\theta = \pi/6$. The spatial dependencies of the pair potentials become very complicated as shown in Fig. 10, where we choose $T_{\rm N}/T_d = 0.01$ for various R. For $R = 0$, the amplitude of Re$[\Delta_{\rm N}(x)]$ is induced toward the inside of N. This situation is similar to the case of $\theta = 0$ by the proximity effect. With the increase of R, the amplitude of Re$[\Delta_d(x)]$ is significantly suppressed at the interface, due to the destructive interference originating from the sign changing nature of $d_{x^2-y^2}$-wave pair potential. The amplitude of Re$[\Delta_{\rm N}(x)]$ is suppressed due to the reduction of the proximity effect. On the other hand, amplitudes of Im$[\Delta_d(x)]$, Re$[\Delta_s(x)]$, and Im$[\Delta_s(x)]$ are enhanced. As regards the subdominant components, the amplitude of Im$[\Delta_s(x)]$ for lower transparent cases $R = 0.75$ and $R = 1$, is one order larger than those of Im$[\Delta_d(x)]$, and Re$[\Delta_s(x)]$ [see Fig. 10(b)]. In particular, for $R = 0.75$, the situation that the amplitude of Im$[\Delta_{\rm N}(x)]$ is induced near the interface of N side is similar to the case of $\theta = \pi/4$. Subdominant components which break TRS is induced also by the proximity effect and depends on the transparencies of the junction.

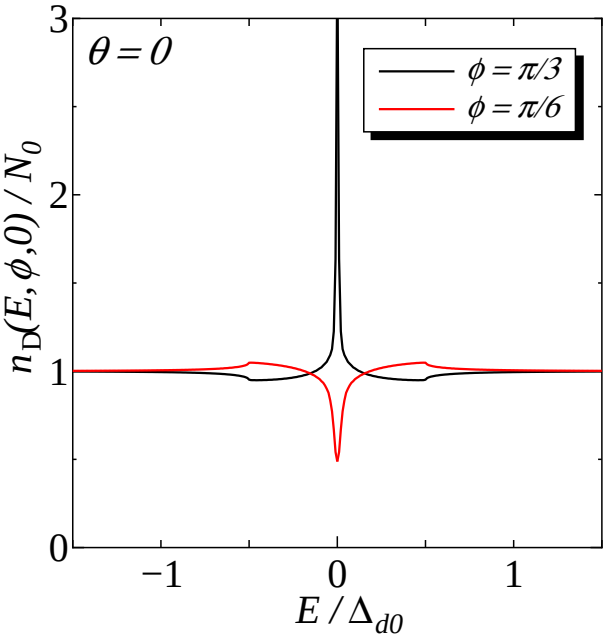

FIG. 9: Angle resolved LDOS at the interface for $\theta = 0$ and $R = 0$.

The corresponding LDOS for $\theta = \pi/6$ are plotted in Figs. 11(a) and 11(b). Here, we choose $T_{\rm N}/T_d = 0.01$, which is the same parameters used in Fig. 10. The resulting line shapes of LDOS are complex reflecting on the complicated spatial dependence of the pair potentials. For $R = 0$, we can see that the zero energy states are formed at the interface and the resulting LDOS has a ZEP due to the *proximity effect*. This ZEP, the origin of which is similar to the case of $\theta = 0$ [see Fig. 6(b)], arises from the sign change of the pair potentials between Re$[\Delta_{\rm N}(x)]$ and Re$[\Delta_{d,s}(x)]$ through Andreev reflections due to proximity effect. With the increase of R, the LDOS has a rather broad ZEP. due to the formation of *ABS's*. This ZEP for intermediate value of R originates from the formation of ABS's peculiar to unconventional superconductors[8,12], *i.e.* with sign change of the pair potentials between $\Delta_d(\phi_+, 0)$ and $\Delta_d(\phi_-, 0)$. With the further increase of R, (see the curve with $R = 0.75$), since the imaginary components of both $\Delta_{\rm N}(x)$ and $\Delta_s(x)$ are induced in the vicinity of the interface, the line shape of the LDOS has a complicated structure reflecting on the complex spatial dependence of pair potentials. For $R = 1$, the LDOS has the ZEP splitting due to the existence of subdominant s-wave component which breaks TRS in the D side, *i.e.*, Im$[\Delta_s(x)]$. As a results, in the N/D junctions with $\theta = \pi/6$, we can conclude that the line shapes of the LDOS around zero energy change from (I) *the ZEP due to proximity effect*, (II) *the ZEP due to the ABS*, and (III) *the ZEP splitting due to the formation of the BTRSS*, with the increase of the magnitude of R.

Finally, we look at the angle resolved LDOS $n_{\rm D}(E, \phi, x)$ in order to understand the basic features of

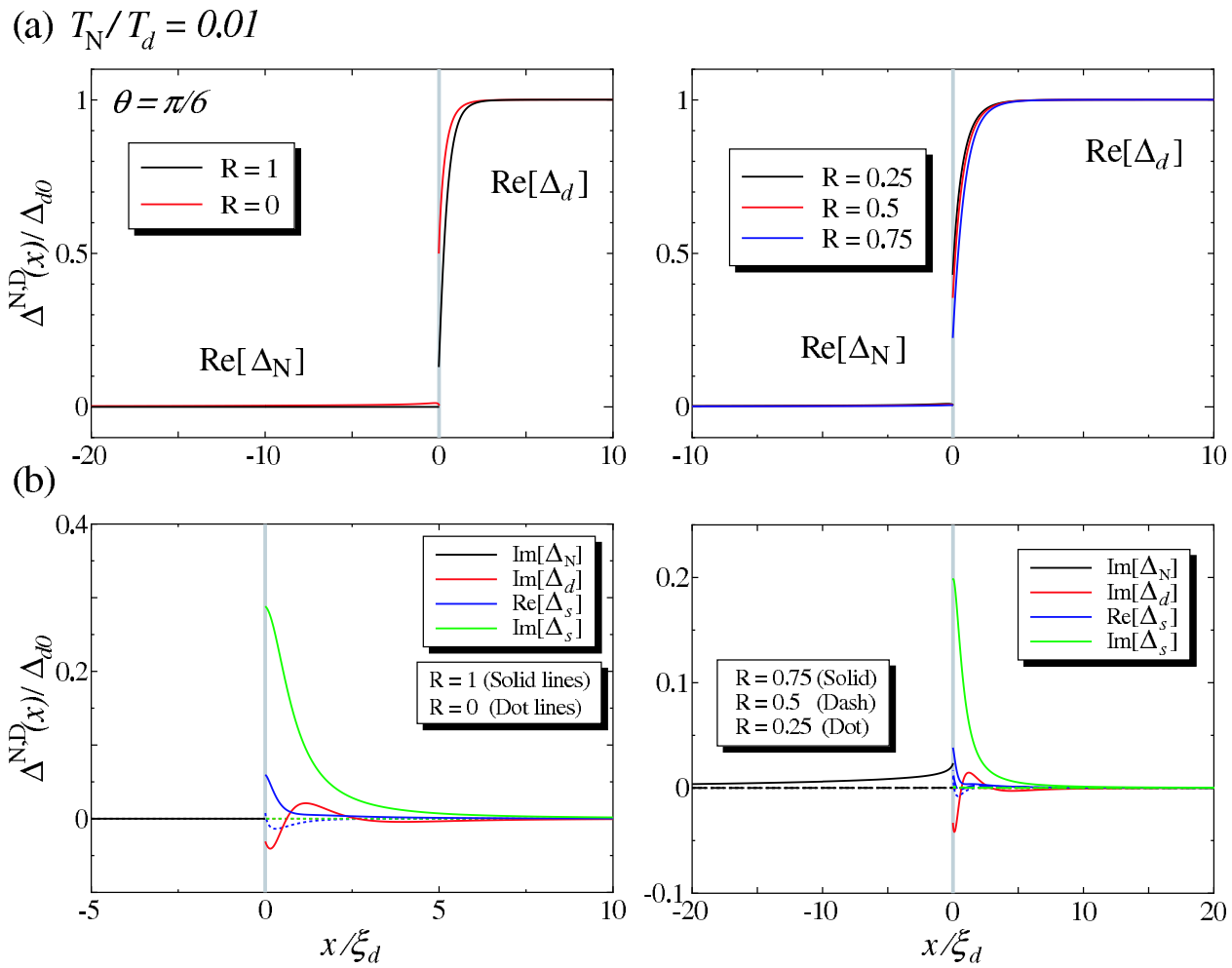

FIG. 10: Spatial dependencies of the pair potentials for the N/D junctions with $\theta = \pi/6$ and $T_N/T_d = 0.01$. In (a), Re[$\Delta_N(x)$], Re[$\Delta_d(x)$], and in (b), Im[$\Delta_N(x)$], Im[$\Delta_d(x)$], Re[$\Delta_s(x)$], Im[$\Delta_s(x)$], are plotted, respectively.

the line shapes of $N_D(E,0)$. In Figs. 12 and 13, the angle resolved LDOS $n_D(E,\phi,x)$ at the interface is plotted for $\theta = \pi/6$ and $R = 0.75$. In order to understand the role of the induced pair potential in N region, we intentionally neglect the pair potential $\Delta_N(x)$ in the N side in the actual calculation of LDOS as shown in the upper panel of Fig. 12 and Fig. 13. We also consider the case, where induced s-wave component $\Delta_s(x)$ is neglected in the calculation of LDOS. First we concentrate on the upper panels where $\Delta_N(x)$ is absent. If only the pure $d_{x^2-y^2}$-wave component exists in the D side, the quasiparticles form the ABS's at zero energy. For $\phi = \pm\pi/3$, since $\Delta_d(\phi_+,0)\Delta_d(\phi_-,0) < 0$ is satisfied, $n_D(E,\phi,0)$ has the ZEP [see Figs. 12(a) and 12(b)]. In the presence of the subdominant s-wave component which breaks TRS in the D side, the resulting $n_D(E,\phi,0)$ is modified. In this case, the line shape of $n_D(E,\phi,0)$ is not asymmetric around $E = 0$, *i.e.*, where $n_D(E,\phi,0) \neq n_D(-E,\phi,0)$, due to the formation of the BTRSS. Therefore, the peak position of $n_D(E,\phi,0)$ is shifted from zero energy. On the other hands, for $\phi = \pm\pi/20$, as $\Delta_d(\phi_+,0)\Delta_d(\phi_-,0) > 0$ is satisfied, $n_D(E,\phi,0)$ has gap structures [see Figs. 13(a) and 13(b)]. These results are consistent with those by Matsumoto and Shiba.[54] Next, we look at lower panels of Figs. 12 and 13. Since induced Im[$\Delta_N(x)$] breaks time reversal symmetry, the resulting line shape of LDOS is no more symmetric around $E = 0$, even for $\Delta_s(x) = 0$. As shown in the lower panels, the presence of $\Delta_N(x)$ forms a minigap around zero energy $E = 0$.

In Fig. 14, the LDOS $n_D(E,\phi,0)$ is plotted for $R = 0$, where the Andreev reflection only exists. In this case, the line shape of the LDOS can be understood only by taking into account the pair potentials $\Delta_N(x)$ and $\Delta_d(x)$. For $\phi = \pi/3$ and $\phi = \pm\pi/20$, the LDOS has no ZEP since $\Delta_N(\phi_+,0)\Delta_d(\phi_+,0) > 0$ is satisfied. The resulting $n_D(E,\phi,0)$ has a gap structure [see Figs. 14(a) and 14(b)]. If the quasiparticle's scattering feel different sign of the pair potentials between the N and D sides, we can expect that the $n_D(E,\phi,0)$ has the ZEP even for $R = 0$. For $\phi = -\pi/3$, since $\Delta_N(\phi_+,0)\Delta_d(\phi_+,0) < 0$ is satisfied, then the $n_D(E,\phi,0)$ has the ZEP [see Fig. 14(b)]. These situations are similar to those studied in Sec. III B.

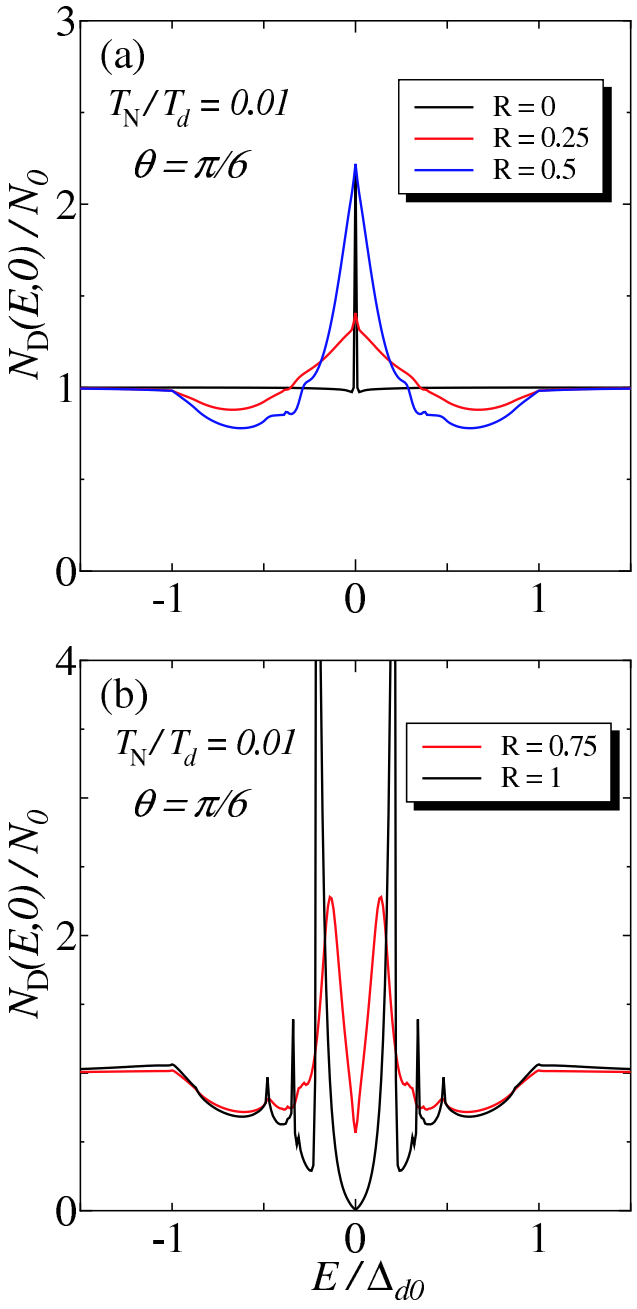

FIG. 11: The LDOS for the N/D junctions with $\theta = \pi/6$ and $T_N/T_d = 0.01$. (a) $R = 0$, 0.25, and 0.5, (b) $R = 0.75$ and 1.

IV. CONCLUSIONS

In this paper, we have studied quasiparticle properties in the N/D junctions, in the presence of the proximity effect as well as the BTRSS in the D side. We assume the attractive interelectron potentials which induces subdominant s-wave components both in the N and D sides. The spatial dependencies of the pair potentials in the N/D junctions are determined self-consistently. The LDOS at the interface of the N/D junctions are studied in detail by changing orientational angle θ and the transparency of the junction. Our main results are summarized as follows.

i) For (110) oriented junction with $\theta = \pi/4$, the predominant $d_{x^2-y^2}$-wave component in the D side is reduced at the interface. The subdominant s-wave component which breaks TRS appears near the (110) interface in low transparent cases. In the N side, subdominant imaginary s-wave component is induced near the interface[62]. The resulting LDOS at the interface in the N side has the ZEP or its splitting depending on the transparency of the junction. These results are consistent with previous theoretical works.[11,53,54,59,62]

ii) For (100) oriented junction, the subdominant s-wave component becomes real number and does not break TRS[62]. With the increase of the transparency of the junction, the magnitude of the s-wave component in the N side is enhanced by the proximity effect. For fully transparent case, the LDOS has very sharp ZEP due to the formation of zero energy states. This ZEP originates from the fact that quasiparticles feel different sign of the pair potentials between the N and D sides through Andreev reflection.

iii) For $\theta = \pi/6$, the spatial dependencies of the pair potentials become very complicated. The resulting LDOS has a wide variety. For high barrier limit, the LDOS has the ZEP splitting.

In the light of our results, although the penetration of the pair potential into the N side by the proximity effect is expected for (100) oriented junctions, the subdominant s-wave components both in the N and D sides are real numbers. Thus, the BTRSS is not formed in the (100) junctions. The present results are inconsistent with previous prediction based on tunneling experiment on high-T_c cuprates by Kohen *et al.*[60] In order to understand their experimental results, we must seek for other possibilities.

In the present paper, we study proximity effect in N/D junctions in the ballistic limit. In the actual junctions, we can not neglect impurity scattering effect. To reply this issue, two of the present author present theoretical works of charge transport in N/D junctions in the presence of the ABS where the N region is a diffusive metal.[26,70] It is an interesting problem to extend the present theory in the diffusive regime based on the Keldysh Green's function formalism.[70] Although there are many works about ABS's in unconventional superconductor junctions up to now,[71,72,73,74,75,76,77,78,79,80,81,82,83,84,85,86,87,88,89,90,91,92,93,94,95,96,97,] proximity effects both in the presence of induced pair potential in the N region and the ABS's are not fully studied. Recent study by Löfwander is remarkable where the proximity effect is studied in the presence of both impurity scattering and induced subdominant component of the pair potentials.[62] Based on his detailed calculation, for (100) junction, a real combination of the proximity effect is always found. For (110) orientation, the s-wave component induced by the proximity effect in the N side breaks TRS.[28,62] These results are consistent

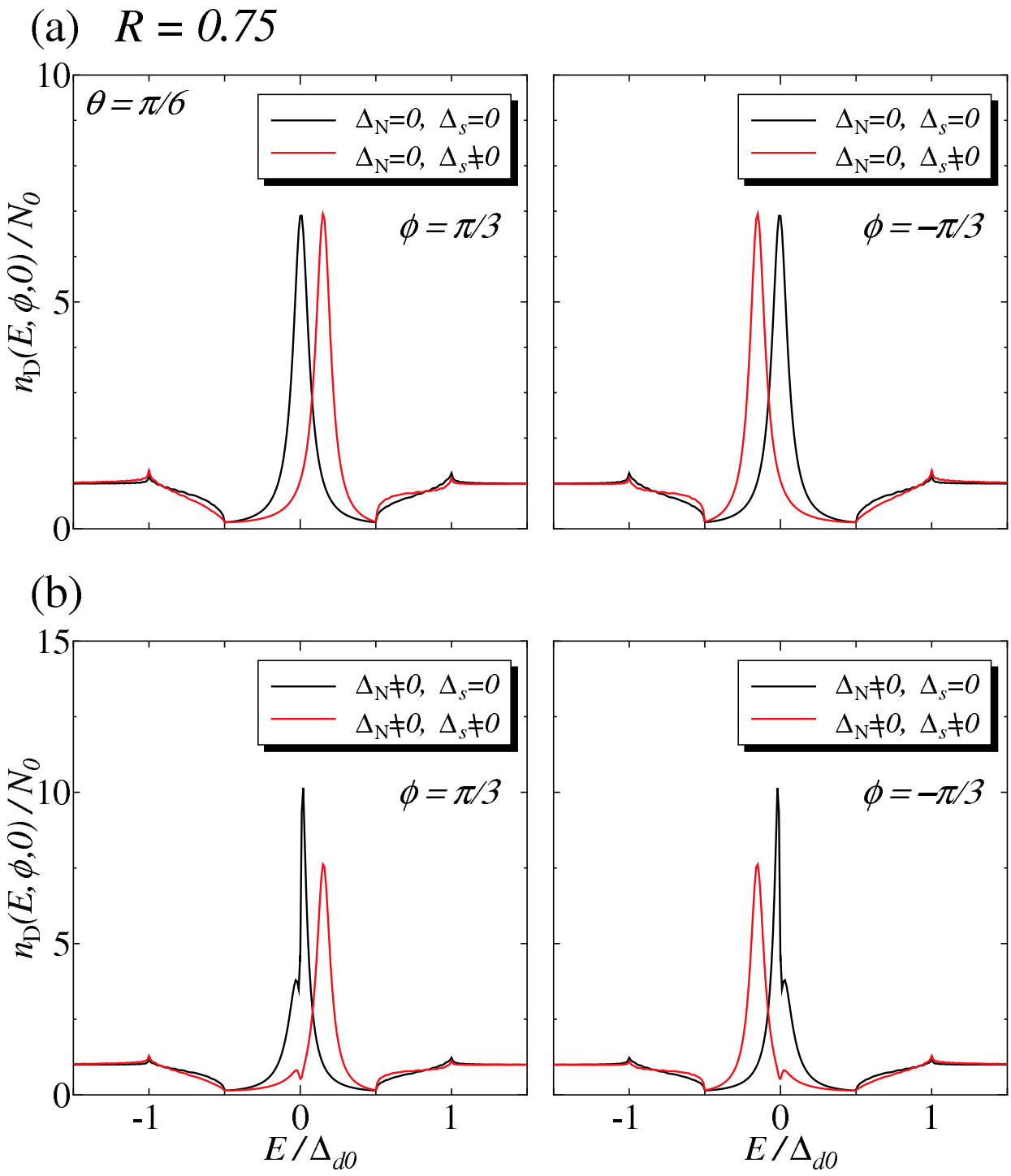

FIG. 12: The angle resolved LDOS $n_{\rm D}(E,\phi,x)$ at the interface with $\theta=\pi/6$ and $R=0.75$. (a): LDOS without subdominant s-wave pair potential in the N side. (b): LDOS in the presence of subdominant s-wave pair potential in the N side. $\phi=\pi/3$ for the left panel and $\phi=-\pi/3$ for the right panel.

with the present results.

As a future problem, to clarify the charge transport property in Josephson junctions both in the presence of ABS[104,105,106,107,108,109,110,111,112,113,114,115,116,117,118,119,120,121,122] and proximity effect is interesting. We want to extend the present theory towards these directions.

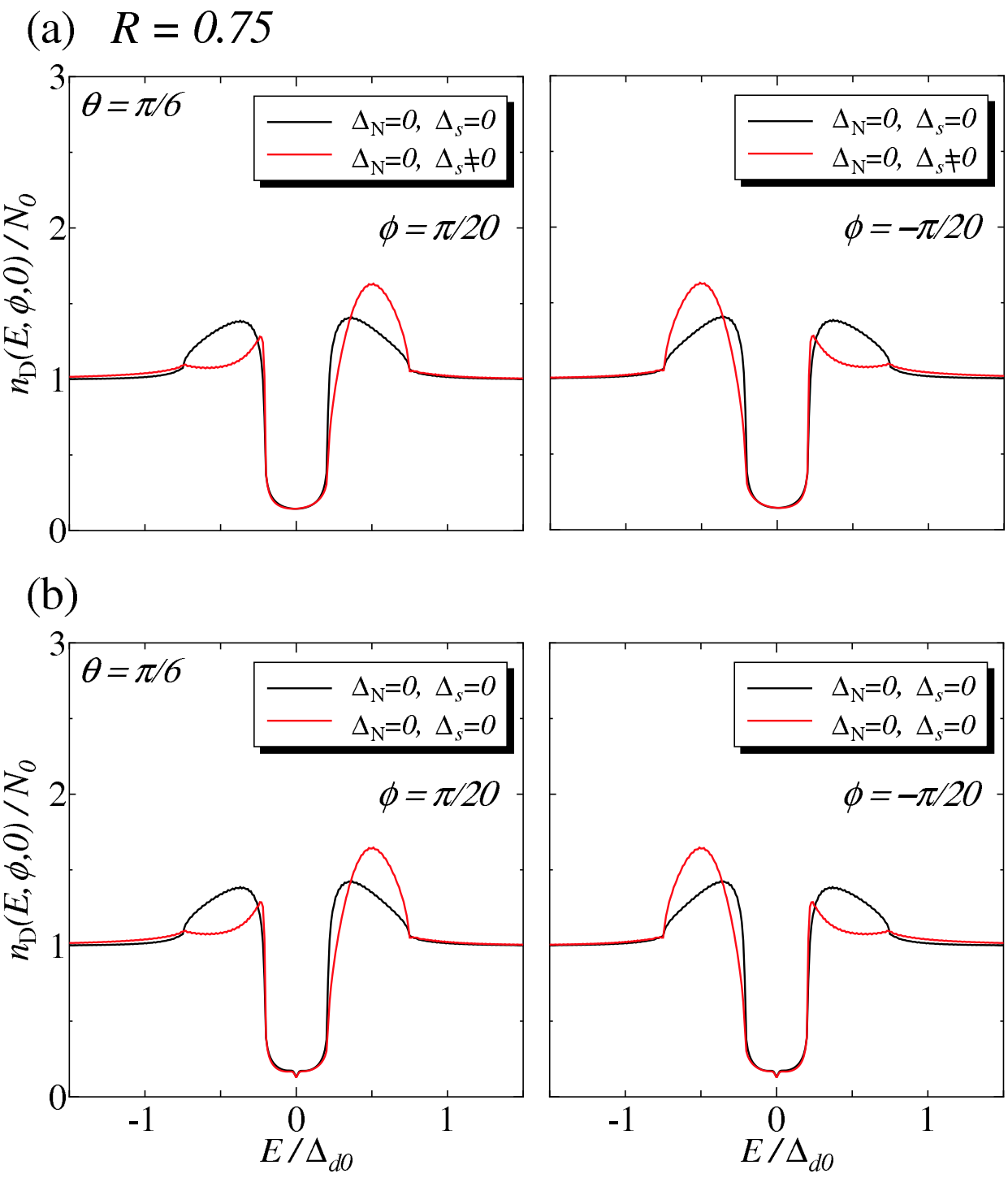

FIG. 13: The angle resolved LDOS $n_{\rm D}(E,\phi,x)$ at the interface with $\theta=\pi/6$ and $R=0.75$. (a): LDOS without subdominant s-wave pair potential in the N side. (b): LDOS in the presence of subdominant s-wave pair potential in the N side. $\phi=\pi/20$ for the left panel and $\phi=-\pi/20$ for the right panel.

Acknowledgments

We would like to sincerely thank Dr. T. Löfwander for critical reading of the manuscript and valuable discussions. The computations have been performed at the Supercomputer Center of Yukawa Institute for Theoretical Physics, Kyoto University.

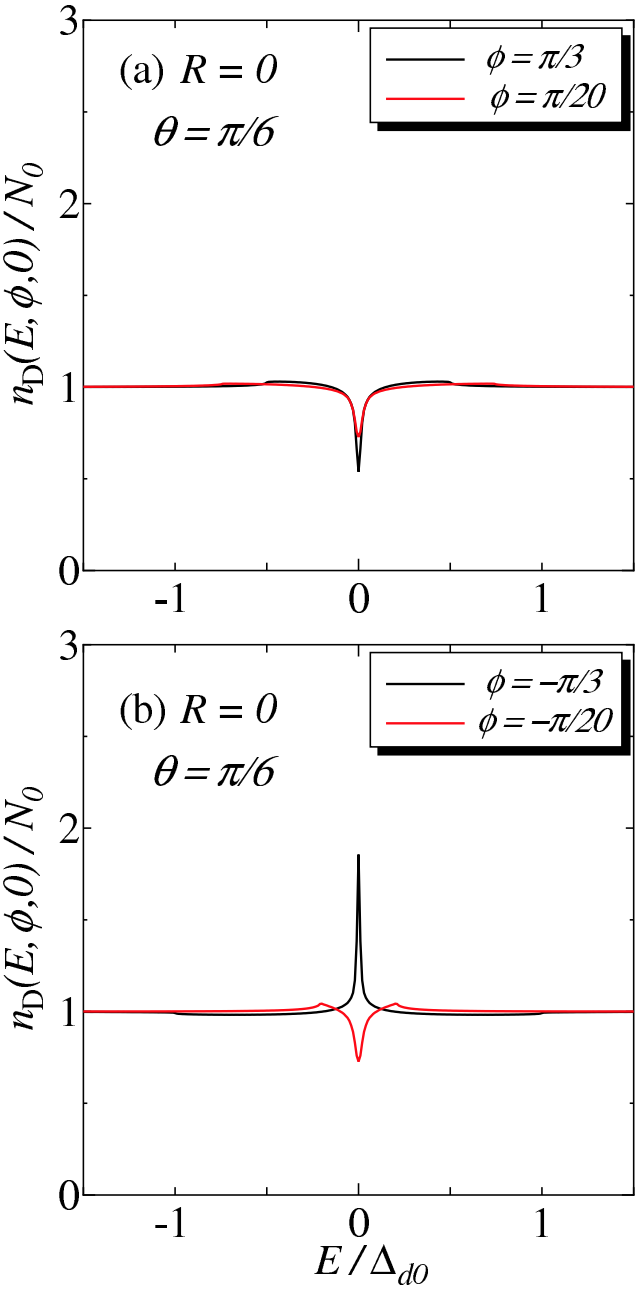

FIG. 14: The angle resolved LDOS $n_{\rm D}(E,\phi,x)$ at the interface with $\theta=\pi/6$ and $R=0$. (a) $\phi=\pi/3$, $\pi/20$, and (b) $\phi=-\pi/3$, $-\pi/20$.

APPENDIX A: BOGOLIUBOV-DE GENNES EQUATION AND QUASI-CLASSICAL APPROXIMATION

Our theoretical formalism is started from the Bogoliubov-de Gennes (BdG) equation for unconventional spin-singlet superconductors,

$$E_n\tilde{u}_n(\boldsymbol{r}) = H_0\tilde{u}_n(\boldsymbol{r}) + \int d\boldsymbol{r}'\Delta(\boldsymbol{r},\boldsymbol{r}')\tilde{v}_n(\boldsymbol{r}'), \tag{A1}$$

$$E_n\tilde{v}_n(\boldsymbol{r}) = -H_0\tilde{v}_n(\boldsymbol{r}) + \int d\boldsymbol{r}'\Delta(\boldsymbol{r},\boldsymbol{r}')^*\tilde{u}_n(\boldsymbol{r}'), \tag{A2}$$

$$H_0 = -\frac{\hbar^2}{2m}\nabla^2 - \mu,$$

where μ is the chemical potential, while $\tilde{u}_n(\boldsymbol{r})$ and $\tilde{v}_n(\boldsymbol{r})$ denote the electron like and holelike components of the wave function

$$\tilde{\Psi}_n(\boldsymbol{r}) = \begin{pmatrix} \tilde{u}_n(\boldsymbol{r}) \\ \tilde{v}_n(\boldsymbol{r}) \end{pmatrix}, \\ \equiv \begin{pmatrix} u_n(\hat{\boldsymbol{k}},\boldsymbol{r}) \\ v_n(\hat{\boldsymbol{k}},\boldsymbol{r}) \end{pmatrix} e^{{\rm i}k_{\rm F}\hat{\boldsymbol{k}}\cdot\boldsymbol{r}} = \Psi_n(\hat{\boldsymbol{k}},\boldsymbol{r})e^{{\rm i}k_{\rm F}\hat{\boldsymbol{k}}\cdot\boldsymbol{r}}. \tag{A3}$$

Here the quantities $\hat{\boldsymbol{k}}$ and $\boldsymbol{r}$ stand for the unit vector of the wave number of the Cooper pair which is fixed on the Fermi surface ($\hat{\boldsymbol{k}}=\boldsymbol{k}_{\rm F}/|\boldsymbol{k}_{\rm F}|$), and the position of the center of mass of Cooper pair, respectively. After applying the quasi-classical approximation, the BdG equation is reduced to the Andreev equation[7,67,68],

$$E_n\Psi_n(\hat{\boldsymbol{k}},\boldsymbol{r}) = -\left[{\rm i}\hbar v_{\rm F}\hat{\boldsymbol{k}}\cdot\nabla + \hat{\Delta}(\hat{\boldsymbol{k}},\boldsymbol{r})\right]\hat{\tau}_3\Psi_n(\hat{\boldsymbol{k}},\boldsymbol{r}), \tag{A4}$$

$$\hat{\Delta}(\hat{\boldsymbol{k}},\boldsymbol{r}) = \begin{pmatrix} 0 & \Delta(\hat{\boldsymbol{k}},\boldsymbol{r}) \\ -\Delta(\hat{\boldsymbol{k}},\boldsymbol{r})^* & 0 \end{pmatrix}. \tag{A5}$$

The wave function $\Psi_n(\hat{\boldsymbol{k}},\boldsymbol{r})$ is obtained by neglecting the rapidly oscillating plane-wave part following the quasi-classical approximation[67,68]. The $\hat{\boldsymbol{k}}$ dependence of $\Delta(\hat{\boldsymbol{k}},\boldsymbol{r})$ represents the symmetry of the pair potential.

In the present study, we consider the case where a secularly reflecting surface or interface runs along the y direction. Then, the pair potential depends only on x since the system is homogeneous along the y direction. The wave function $\Psi_n(\hat{\boldsymbol{k}},\boldsymbol{r})$ can be written in the following directional notation:[53,65]

$$\Psi_n(\hat{\boldsymbol{k}},x,y) = \Big[\Phi_n^{(+)}(\phi_+,x)e^{{\rm i}|k_{{\rm F}x}|x} \\ + \Phi_n^{(-)}(\phi_-,x)e^{-{\rm i}|k_{{\rm F}x}|x}\Big]e^{{\rm i}|k_{{\rm F}y}|y},$$

$$\Phi_n^{(\alpha)}(\phi_\alpha,x) = \begin{pmatrix} u_n^{(\alpha)}(\phi_\alpha,x) \\ v_n^{(\alpha)}(\phi_\alpha,x) \end{pmatrix}. \tag{A6}$$

Here $\pm$ represents the sign of the x component of the Fermi wave number $k_{{\rm F}x}$ and $\alpha(\beta)=\pm$. We define a Green's function $G_{\alpha\beta}(\phi,x,x')$ and a quasi-classical Green's function $g_{\alpha\beta}(\phi,x)$

$$G_{\alpha\beta}(\phi,x,x') = \sum_n \frac{\Phi_n^{(\alpha)}(\phi_\alpha,x)\Phi_n^{(\beta)}(\phi_\beta,x')^\dagger}{{\rm i}\omega_m - E_n}, \tag{A7}$$

$$g_{\alpha\beta}(\phi,x) \pm {\rm i}(\hat{\gamma}_3)_{\alpha\beta} = -2\hbar|v_{{\rm F}x}|\hat{\tau}_3 G_{\alpha\beta}(\phi,x\pm 0,x). \tag{A8}$$

where $\hat{\gamma}_3$ is the Pauli matrix in the directional space[65].

APPENDIX B: EVOLUTION OPERATOR $\tilde{U}^l_\alpha(\phi_\alpha, x, x')$

The quasi-classical Green's function can be written by the following evolution operator $U_\alpha(\phi_\alpha, x, x')$ as

$$g_{\alpha\beta}(\phi, x) = U_\alpha(\phi_\alpha, x, x') g_{\alpha\beta}(\phi, x') U^{-1}_\beta(\phi_\beta, x, x'), \quad \text{(B1)}$$

where $U_\alpha(\phi_\alpha, x, x')$ satisfies the Andreev equation

$$\begin{aligned} &\mathrm{i}\hbar|v_{\mathrm{F}x}|\frac{\partial}{\partial x}U_\alpha(\phi_\alpha, x, x') \\ &\quad = -\alpha\left[\mathrm{i}\omega_m\hat{\tau}_3 + \hat{\Delta}(\phi_\alpha, x)\right] U_\alpha(\phi_\alpha, x, x'), \end{aligned} \quad \text{(B2)}$$

with $U_\alpha(\phi_\alpha, x, x) = 1$.

Hence, the evolution operators in the l side can be divided into a growing part and a decaying part

$$\begin{aligned} U^l_\alpha(\phi_\alpha, x, x') =& \Lambda^{l(+)}_\alpha(\phi_\alpha, x, x') e^{\kappa^l_\alpha(x-x')} \\ &+ \Lambda^{l(-)}_\alpha(\phi_\alpha, x, x') e^{-\kappa^l_\alpha(x-x')}, \end{aligned} \quad \text{(B3)}$$

$$\begin{aligned} \Lambda^{l(+)}_\alpha(\phi_\alpha, x, x') =& -\frac{1}{W^l_\alpha}\Phi^{l(+)}_n(\phi_\alpha, x)^{\mathrm{T}}\Phi^{l(-)}_n(\phi_\alpha, x')\hat{\tau}_2, \\ \Lambda^{l(-)}_\alpha(\phi_\alpha, x, x') =& \frac{1}{W^l_\alpha}\Phi^{l(-)}_n(\phi_\alpha, x)^{\mathrm{T}}\Phi^{l(+)}_n(\phi_\alpha, x')\hat{\tau}_2, \end{aligned} \quad \text{(B4)}$$

where

$$\kappa^l_\alpha = \frac{\Omega^l_\alpha}{|v_{\mathrm{F}x}|}, \quad \Omega^l_\alpha = \sqrt{\omega_m^2 + |\Delta^l(\phi_\alpha, \infty)|^2}, \quad \text{(B5)}$$

$$\begin{aligned} W^l_\alpha &= {}^{\mathrm{T}}\Phi^{l(+)}_n(\phi_\alpha, x)\hat{\tau}_2\Phi^{l(-)}_n(\phi_\alpha, x) \\ &= -{}^{\mathrm{T}}\Phi^{l(-)}_n(\phi_\alpha, x)\hat{\tau}_2\Phi^{l(+)}_n(\phi_\alpha, x) \\ &= \text{const.} \end{aligned} \quad \text{(B6)}$$

In the above, ${}^{\mathrm{T}}\Phi^{l(\alpha)}_n(\phi_\alpha, x)$ denotes the transposition of $\Phi^{l(\alpha)}_n(\phi_\alpha, x)$. In the actual numerical calculations, we use $\tilde{U}^l_\alpha(\phi_+, x, 0)$ and $\tilde{U}^l_\alpha(\phi_+, 0, x)$ given by

$$\tilde{U}^{\mathrm{N}}_+(\phi_+, x, 0) = U^{\mathrm{N}}_+(\phi_+, x, 0)e^{\kappa^{\mathrm{N}}_+ x}, \quad \text{(B7)}$$

$$\tilde{U}^{\mathrm{D}}_+(\phi_+, 0, x) = U^{\mathrm{D}}_+(\phi_+, 0, x)e^{-\kappa^{\mathrm{D}}_+ x}. \quad \text{(B8)}$$

APPENDIX C: FOR AVOIDING DIVERGENCE IN OUR CALCULATION

In particular, if $\Delta^{\mathrm{N}}(\phi_+, -\infty)$ $[\Delta^{\mathrm{D}}(\phi_-, \infty)] = 0$, we can find $\mathcal{G}^{\mathrm{N}}_+$ $[\mathcal{G}^{\mathrm{D}}_-] \to \infty$. In this case, instead of Eq. (20), we solve the following equation as

$$\begin{aligned} \hbar|v_{\mathrm{F}x}|\frac{\partial}{\partial x}\left(\frac{1}{\mathcal{G}^l_\alpha(x)}\right) =& -\alpha\left[2\omega_m\left(\frac{1}{\mathcal{G}^l_\alpha(x)}\right)\right. \\ &\left. + \Delta^l(\phi_\alpha, x)^*\left(\frac{1}{\mathcal{G}^l_\alpha(x)}\right)^2 - \Delta^l(\phi_\alpha, x)\right], \end{aligned} \quad \text{(C1)}$$

under initial condition,

$$\frac{1}{\mathcal{G}^l_\alpha(x)} = -\frac{\Delta^l(\phi_\alpha, -\alpha\infty)}{\omega_m + \Omega^l_\alpha}. \quad \text{(C2)}$$

[1] M. Sigrist and T.M. Rice, J. Phys. Soc. Jpn. **61**, 4283 (1992).
[2] M. Sigrist and T.M. Rice, Rev. Mod. Phys. **67**, 505 (1995).
[3] D.J. Scalapino, Phys. Rep. **250**, 329 (1995).
[4] D.J. Van Harlingen, Rev. Mod. Phys. **67**, 515 (1995).
[5] C.C. Tsuei and J.R. Kirtley, Rev. Mod. Phys. **72**, 969 (2001).
[6] L.J. Buchholtz and G. Zwicknagl, Phys. Rev. B **23**, 5788 (1981).
[7] C.R. Hu, Phys. Rev. Lett. **72**, 1526 (1994).
[8] Y. Tanaka and S. Kashiwaya, Phys. Rev. Lett. **74**, 3451 (1995),
[9] S. Kashiwaya, Y. Tanaka, M. Koyanagi, H. Takashima, and K. Kajimura, Phys. Rev. B **51**, 1350 (1995).
[10] M. Matsumoto and H. Shiba, J. Phys. Soc. Jpn. **64**, 3384 (1995).
[11] M. Fogelström, D. Rainer, and J.A. Sauls, Phys. Rev. Lett. **79**, 281 (1997).
[12] S. Kashiwaya and Y. Tanaka, Rep. Prog. Phys. **63**, 1641 (2000).
[13] S. Kashiwaya, Y. Tanaka, M. Koyanagi, and K. Kajimura, Phys. Rev. B **53**, 2667 (1996).
[14] Yu. S. Barash, A. A. Svidzinsky, and H. Burkhardt, Phys. Rev. B **55**, 15282 (1997).
[15] T. Löfwander, V.S. Shumeiko, and G. Wendin, Supercond. Sci. Technol. **14**, R53 (2001).
[16] Y. Asano, Y. Tanaka and S. Kashiwaya, Phys. Rev. B **69**, 134501 (2004).
[17] Y. Tanuma, Y. Tanaka, M. Yamashiro, and S. Kashiwaya, Phys. Rev. B **57**, 7997 (1998).
[18] Y. Tanuma, Y. Tanaka, M. Ogata, and S. Kashiwaya, J. Phys. Soc. Jpn. **67**, 1118 (1998).
[19] Y. Tanuma, Y. Tanaka, M. Ogata, and S. Kashiwaya, Phys. Rev. B **60**, 9817 (1999).
[20] J. X. Zhu and C. S. Ting, Phys. Rev. B **59**, R14165 (1999).
[21] K.V. Samokhin and M.B. Walker, Phys. Rev. B **64**,

172506 (2001).
[22] P. Pairor and M.B. Walker Phys. Rev. B **65**, 064507 (2002).
[23] Y. Asano and Y. Tanaka, Phys. Rev. B **65**, 064522 (2002).
[24] Y. Asano, Y. Tanaka, and S. Kashiwaya. Phys. Rev. B **69**, 214509 (2004).
[25] Y. Tanaka, Y. Tanuma, and S. Kashiwaya, Phys. Rev. B **64**, (2001) 054510.
[26] Y. Tanaka, Yu.V. Nazarov, and S. Kashiwaya, Phys. Rev. Lett. **90**, (2003) 167003.
[27] Y. Tanaka, A.A. Golubov, and S. Kashiwaya, Phys. Rev. B **68**, 054513 (2003).
[28] N. Kitaura, H. Itoh, Y. Asano, Y. Tanaka, J. Inoue, Y. Tanuma, and S. Kashiwaya, J. Phys. Soc. Jpn. **72**, 1718 (2003).
[29] A.A. Golubov and M.Y. Kupriyanov, Pis'ma Zh. Eksp. Teor. fiz **67**, 478 (1998) [Sov. Phys. JETP Lett. **67**, 501 (1998)].
[30] A.A. Golubov and M.Y. Kupriyanov, Pis'ma Zh. Eksp. Teor. fiz **69**, 242 (1999) [Sov. Phys. JETP Lett. **69**, 262 (1999)].
[31] A. Poenicke, Yu.S. Barash, C. Bruder, and V. Istyukov, Phys. Rev. B **59**, 7102 (1999).
[32] K. Yamada, Y. Nagato, S. Higashitani, and K. Nagai, J. Phys. Soc. Jpn. **65**, 1540 (1996).
[33] T. Lück, U. Eckern, and A. Shelankov, Phys. Rev. B **63**, 064510 (2002).
[34] I. Lubimova and G. Koren, Phys. Rev. B **68**, 224519 (2003).
[35] J. Geerk, X.X. Xi, and G. Linker, Z. Phys. B. **73**, 329 (1988).
[36] J. Lesueur, L.H. Greene, W.L. Feldman, and A. Inam, Physica C **191**, 325 (1992).
[37] S. Kashiwaya, Y. Tanaka, M. Koyanagi, H. Takashima, and K. Kajimura, Phys. Rev. B **51**, 1350 (1995).
[38] L. Alff, H. Takashima, S. Kashiwaya, N. Terada, H. Ihara, Y. Tanaka, M. Koyanagi, and K. Kajimura, Phys. Rev. B **55**, R14757 (1997).
[39] M. Covington, M. Aprili, E. Paraoanu, L.H. Greene, F. Xu, J. Zhu, and C.A. Mirkin, Phys. Rev. Lett. **79**, 277 (1997).
[40] H. Aubin, L. H. Greene, Sha Jian, and D. G. Hinks, Phys. Rev. Lett. **89**, 177001 (2002).
[41] J.Y.T. Wei, N.-C. Yeh, D.F. Garrigus, and M. Strasik, Phys. Rev. Lett. **81**, 2542 (1998).
[42] I. Iguchi, W. Wang, M. Yamazaki, Y. Tanaka, and S. Kashiwaya, Phys. Rev. B **62**, R6131 (2000).
[43] Y. Dagan and G. Deutscher, Phys. Rev. Lett. **87**, 177004 (2001).
[44] A. Sharoni, O. Millo, A. Kohen, Y. Dagan, R. Beck, G. Deutscher, and G. Koren, Phys. Rev. B **65**, 134526 (2002).
[45] G. Koren, L. Shkedy, and E. Polturak, cond-mat/0306594 (2003).
[46] S. Kashiwaya, Y. Tanaka, N. Terada, M. Koyanagi, S. Ueno, L. Alff, H. Takashima, Y. Tanuma, and K. Kajimura, J. Phys. Chem. Solids. **59**, 2034 (1998).
[47] J.W. Ekin, Y. Xu, S. Mao, T. Venkatesan, D.W. Face, M. Eddy, and S. A. Wolf, Phys. Rev. B **56**, 13746 (1997).
[48] A. Biswas, P. Fournier, M.M. Qazilbash, V.N. Smolyaninova, H. Balci, and R.L. Greene, Phys. Rev. Lett. **88**, 207004 (2002).
[49] M.M. Qazilbash, A. Biswas, Y. Dagan, R.A. Ott, and R.L. Greene, Phys. Rev. B **68**, 024502 (2003).
[50] M. Sigrist, D. B. Bailey, and R. B. Laughlin, Phys. Rev. Lett. **74**, 3249 (1995).
[51] K. Kuboki and M. Sigrist, J. Phys. Soc. Jpn. **65**, 361 (1996).
[52] M. Sigrist, Prog. Theo. Phys. **99**, 899 (1998).
[53] M. Matsumoto and H. Shiba, J. Phys. Soc. Jpn. **64**, 4867 (1995).
[54] M. Matsumoto and H. Shiba, J. Phys. Soc. Jpn. **65**, 2194 (1996).
[55] K. Krishana, N. P. Ong, Q. Li, G. D. Gu, and N. Koshizuka, Science **277**, 83 (1997).
[56] A. V. Balatsky, Phys. Rev. Lett. **80**, 1972 (1998).
[57] R. B. Laughlin, Phys. Rev. Lett. **80**, 5188 (1998).
[58] W.K. Neils and D.J. Van Harlingen, Phys. Rev. Lett. **88**, 047001 (2002).
[59] Y. Tanuma, Y. Tanaka, and S. Kashiwaya, Phys. Rev. B **64**, 214519 (2001).
[60] A. Kohen, G. Leibovitch, and G. Deutscher, Phys. Rev. Lett. **90**, 207005 (2003).
[61] Y. Ohashi, J. Phys. Soc. **65**, 823 (1996).
[62] T. Löfwander, Phys. Rev. B **70**, 094518 (2004).
[63] G. Eilenberger, Z. Phys. **214**, 195 (1968).
[64] K. Nagai, *Quasiclassical Methods in Superconductivity and Superfluidity*, edited by D. Rainer and J.A. Sauls (unpublished).
[65] M. Ashida, S. Aoyama, J. Hara, and K. Nagai, Phys. Rev. B **40**, 8673 (1989).
[66] Y. Nagato, K. Nagai, and J. Hara, J. Low Temp. Phys. **93**, 33 (1993).
[67] C. Bruder, Phys. Rev. B **41**, 4017 (1990).
[68] J. Kurkijärvi and D. Rainer, *Helium Three*, edited by W. P. Halperin and L. P. Pitaevskii (Elsevier, Amsterdam, 1990).
[69] Y. Tanaka and S. Kashiwaya, Phys. Rev. B **53** 9371 (1996).
[70] Y. Tanaka, Y.V. Nazarov, A.A. Golubov, and S. Kashiwaya, Phys. Rev. B **69** 144519 (2004), Y. Tanaka and S. Kashiwaya, Phys. Rev. B **70** 012507 (2004).
[71] M. Yamashiro, Y. Tanaka, and S. Kashiwaya, Phys. Rev. B **56**, 7847 (1997).
[72] M. Yamashiro, Y. Tanaka, and S. Kashiwaya, J. Phys. Soc. Jpn. **67**, 3364 (1998).
[73] M. Yamashiro, Y. Tanaka Y. Tanuma, and S. Kashiwaya, J. Phys. Soc. Jpn. **67**, 3224 (1998).
[74] M. Yamashiro, Y. Tanaka Y. Tanuma, and S. Kashiwaya, J. Phys. Soc. Jpn. **68**, 2019 (1999).
[75] C. Honerkamp and M. Sigrist, Prog. Theor. Phys. **100**, 53 (1998).
[76] C. Honerkamp and M. Sigrist, J. Low Temp. Phys. **111**, 895 (1998).
[77] Y. Tanaka, T. Asai, N. Yoshida, J. Inoue, and S. Kashiwaya, Phys. Rev. B **61**, R11902 (2000).
[78] Y. Tanaka, T. Hirai, K. Kusakabe, and S. Kashiwaya, Phys. Rev. B **60**, 6308 (1999).
[79] T. Hirai, K. Kusakabe, and Y. Tanaka, Physica C **336**, 107 (2000).
[80] K. Kusakabe and Y. Tanaka, Physica C **367**, 123 (2002).
[81] K. Kusakabe and Y. Tanaka, J. Phys. Chem. Solids **63**, 1511 (2002).
[82] N. Stefanakis, Phys. Rev. B **64**, 224502 (2001).
[83] Z.C. Dong, D.Y. Xing, and Jinming Dong, Phys. Rev. B **65**, 214512 (2002).
[84] Z.C. Dong, D.Y. Xing, Z.D. Wang, Ziming Zheng, and Jinming Dong, Phys. Rev. B **63**, 144520 (2001).
[85] Yu.S. Barash, M.S. Kalenkov, and J. Kurkijärvi, Phys.

Rev. B **62**, 6665 (2000).
[86] M.H.S. Amin, A.N. Omelyanchouk, and A.M. Zagoskin, Phys. Rev. B **63**, 212502 (2001).
[87] Shin-Tza Wu and Chung-Yu Mou, Phys. Rev. B **66**, 012512 (2002).
[88] J.-X. Zhu, B. Friedman, and C.S. Ting, Phys. Rev. B **59**, 9558 (1999).
[89] S. Kashiwaya, Y. Tanaka, N. Yoshida, and M.R. Beasley, Phys. Rev. B **60**, 3572 (1999).
[90] N. Yoshida, Y. Tanaka, J. Inoue, and S. Kashiwaya, J. Phys. Soc. Jpn. **68**, 1071 (1999).
[91] I. Žutić and O.T. Valls, Phys. Rev. B **60**, 6320 (1999).
[92] T. Hirai, N. Yoshida, Y. Tanaka, J. Inoue, and S. Kashiwaya, J. Phys. Soc. Jpn. **70**, 1885 (2001).
[93] N. Yoshida, H. Itoh, T. Hirai, Y. Tanaka, J. Inoue, and S. Kashiwaya, Phsica C **367**, 135 (2002).
[94] T. Hirai, Y. Tanaka, N. Yoshida, Y. Asano, J. Inoue, and S. Kashiwaya, Phys. Rev. B **67**, 174501 (2003).
[95] K. Sengupta, I. Žutić, H.-J. Kwon, V.M. Yakovenko, and S. Das Sarma, Phys. Rev. B **63**, 144531 (2001).
[96] Y. Tanuma, K. Kuroki, Y. Tanaka, and S. Kashiwaya, Phys. Rev. B **64**, 214510 (2001).
[97] Y. Tanuma, K. Kuroki, Y. Tanaka, R. Arita, S. Kashiwaya, and H. Aoki, Phys. Rev. B **66**, 094507 (2002).
[98] Y. Tanuma, Y. Tanaka, K. Kuroki, and S. Kashiwaya, Phys. Rev. B **66**, 174502 (2002).
[99] Y. Tanuma, K. Kuroki, Y. Tanaka, and S. Kashiwaya, Phys. Rev. B **68**, 214513 (2003).
[100] S. Kashiwaya, Y. Tanaka, M. Koyanagi, and K. Kajimura, J. Phys. Chem. Solids **56**, 1721 (1995).
[101] Y. Tanaka, H. Tsuchiura, Y. Tanuma, and S. Kashiwaya, J. Phys. Soc. Jpn. **71**, 271 (2002).
[102] Y. Tanaka, Y. Tanuma K. Kuroki, and S. Kashiwaya, J. Phys. Soc. Jpn. **71**, 2102 (2002).
[103] Y. Tanaka, H. Itoh, H. Tsuchiura, Y. Tanuma, J. Inoue, and S. Kashiwya, J. Phys. Soc. Jpn. **71**, 2005 (2002).
[104] Y. Tanaka and S. Kashiwaya, Phys. Rev. B **53**, R11957 (1996).
[105] Y. Tanaka and S. Kashiwaya, Phys. Rev. B **56**, 892 (1997).
[106] Y. Tanaka and S. Kashiwaya, Phys. Rev. B **58**, R2948 (1998).
[107] Y. Tanaka and S. Kashiwaya, J. Phys. Soc. Jpn. **68**, 3485 (1999).
[108] Y. Tanaka and S. Kashiwaya, J. Phys. Soc. Jpn. **69**, 1152 (2000).
[109] Yu.S. Barash, H. Burkhardt, and D. Rainer, Phys. Rev. Lett. **77**, 4070 (1996).
[110] H. Hilgenkamp, J. Mannhart, and B. Mayer, Phys. Rev. B **53**, 14586 (1996).
[111] H. Hilgenkamp and J. Mannhart, Rev. Mod. Phys. **74**, 485 (2002).
[112] E. Il'ichev, M. Grajcar, R. Hlubina, R.P.J. Ijsselsteijn, H.E. Hoenig, H.-G. Meyer, A. Golubov, M.H.S. Amin, A.M. Zagoskin, A.N. Omelyanchouk, and M.Y. Kupriyanov, Phys. Rev. Lett. **86**, 5369 (2001).
[113] E. Il'ichev, V. Zakosarenko, R.P.J. Ijsselsteijn, V. Schultze, H.-G. Meyer, H.E. Hoenig, H. Hilgenkamp, and J. Mannhart, Phys. Rev. Lett. **81**, 894 (1998).
[114] F. Lombardi, F. Tafuri, F. Ricci, F. Miletto Granozio, A. Barone, G. Testa, E. Sarnelli, J.R. Kirtley, and C.C. Tsuei, Phys. Rev. Lett. **89**, 207001 (2002).
[115] H.J.H. Smilde, Ariando, D.H.A. Blank, G.J. Gerritsma, H. Hilgenkamp, and H. Rogalla, Phys. Rev. Lett. **88**, 057004 (2002).
[116] T. Imaizumi, T. Kawai, T. Uchiyama, and I. Iguchi, Phys. Rev. Lett. **89**, 017005 (2002).
[117] H. Arie, K. Yasuda, H. Kobayashi, I. Iguchi, Y. Tanaka, and S. Kashiwaya, Phys. Rev. B **62**, 11864 (2000).
[118] Y. Asano, Phys. Rev. B **63**, 052512 (2001).
[119] Y. Asano, Phys. Rev. B **64**, 014511 (2001).
[120] Y. Asano, Phys. Rev. B **64**, 224515 (2001).
[121] Y. Asano, J. Phys. Soc. Jpn. **71**, 905 (2002).
[122] Y. Asano, Y. Tanaka, M. Sigrist, and S. Kashiwaya, Phys. Rev. B **67**, 184505 (2003).